Theor Chem Acc (2010) 125:145–172
DOI 10.1007/s00214-009-0597-x

OVERVIEW

Review of biorthogonal coupled cluster representations for electronic excitation

Jochen Schirmer · Frank Mertins

Received: 14 March 2009 / Accepted: 8 June 2009 / Published online: 2 July 2009

Abstract Single-reference coupled-cluster (CC) methods for electronic excitation are based on a biorthogonal representation (bCC) of the (shifted) Hamiltonian in terms of excited CC states, also referred to as correlated excited (CE) states, and an associated set of states biorthogonal to the CE states, the latter being essentially configuration interaction (CI) configurations. The bCC representation generates a non-hermitian secular matrix, the eigenvalues representing excitation energies, while the corresponding spectral intensities are to be derived from both the left and right eigenvectors. Using the perspective of the bCC representation, a systematic and comprehensive analysis of the excited-state CC methods is given, extending and generalizing previous such studies. Here, the essential topics are the truncation error characteristics and the separability properties, the latter being crucial for designing size-consistent approximation schemes. Based on the general order relations for the bCC secular matrix and the (left and right) eigenvector matrices, formulas for the perturbation-theoretical order of the truncation errors (TEO) are derived for energies, transition moments, and property matrix elements of arbitrary excitation classes and truncation levels. In the analysis of the separability properties of the transition moments, the decisive role of the so-called dual ground state is revealed. Due to the use of CE states, the bCC approach can be compared to so-called intermediate state representation (ISR) methods based exclusively on suitably orthonormalized CE states. As the present analysis shows, the bCC approach has decisive advantages over the conventional CI treatment, but also distinctly weaker TEO and separability properties in comparison to a full (and hermitian) ISR method.

Keywords Electronic excitation · Coupled-cluster methods · Intermediate state representations

1 Introduction

The extension of the coupled-cluster (CC) approach [1–3], originally devised for ground states, to the treatment of electronic excitation has afforded the emergence of a variety of highly successful computational methods, excelling at the potential for both numerical efficiency and accuracy. The excited-state CC methodology comprises three major developments referred to as the coupled-cluster linear response (CCLR) theory [4–8], the equation-of-motion coupled-cluster (EOM-CC) approach [9–14] and the symmetry-adapted cluster configuration interaction (SAC-CI) [15–17]. While these developments vary in the derivation of the CC equations, the resulting computational schemes are largely equivalent. A notable difference, however, is the treatment of transition moments and excited-state properties, where, in contrast to the CC-EOM and SAC-CI schemes, the CCLR theory leads to size-consistent expressions.

The basic feature of the CC methods is the use of so-called correlated excited (CE) states as basis states in the expansion of the exact excited states. These CE states are obtained by applying physical excitation operators associated with single (S), double (D), triple (T), ... electron

Dedicated to Professor Sandor Suhai on the occasion of his 65th birthday and published as part of the Suhai Festschrift Issue.

J. Schirmer (✉) · F. Mertins
Theoretische Chemie, Physikalisch-Chemisches Institut, Universität Heidelberg, 69120 Heidelberg, Germany
e-mail: Jochen.Schirmer@pci.uni-heidelberg.de

excitations to the exact (correlated) CC ground state, $|\Psi_J^0\rangle = \hat{C}_J|\Psi_0^{cc}\rangle$, rather than to the Hartree–Fock (HF) ground state, $|\Phi_J\rangle = \hat{C}_J|\Phi_0\rangle$, establishing in the latter case the familiar configuration interaction (CI) basis states or CI configurations. Obviously, the CE states represent intermediates of sorts, positioned between the simple CI configurations and the exact final states. Accordingly, methods based on the use of CE states have been referred to as intermediate state representations (ISR) [18], and the excited-state CC approach is closely related to the family of ISR methods. However, the CE states are not orthonormal, and this problem is dealt with by introducing, in addition to the CE states, the associated set of biorthogonal states. Using the biorthogonal states on the left side and the CE states on the right-hand side, one obtains a mixed (biorthogonal) representation of the (shifted) Hamiltonian, giving rise to a non-hermitian secular matrix. The two sets of states differ distinctly in their intrinsic quality. In fact, the biorthogonal states can be identified essentially as CI configurations. This means that the biorthogonal CC (bCC) representation represents a hybrid approach, combining the CI and ISR concepts in equal measure.

What are the merits of an ISR approach as compared to the conceptually so much simpler CI treatment? The answer is that the ISR methods are not (or much less) affected by two basic deficiencies of the CI approximation schemes, namely the lack of size consistency and the need for relatively large explicit configuration spaces. The size-consistency error inherent to limited CI treatments [as opposed to full (F) CI expansions] stems from the *non-separable* structure of the CI secular equations. More precisely, for a system composed of non-interacting fragments, there is no a priori decoupling of the CI secular matrix into corresponding fragment blocks. The inevitable and, moreover, uncontrollable size-consistency error associated with truncated CI expansions grows with the system size, rendering the results for extended systems useless. This is why CI cannot rank as a genuine many-body method. Second, large CI expansions (configuration spaces) are needed to suppress the quite unfavorable truncation error, that is, the error due to discarding higher excitation classes in the CI expansions. For example, a CI expansion extending through single and double excitations (CISD) induces a truncation error of second order of perturbation theory (PT) in the excitation energies of singly excited states. In the CC methods, by contrast, the corresponding (SD) truncation error is of third order. Even more advantageous is the situation in full (hermitian) ISR methods, where the SD truncation error is already of the fourth order.

The purpose of this paper is to review the separability properties and truncation error characteristics of the excited-state CC schemes, aiming here at a more systematic and more comprehensive analysis than available so far. Previous studies of this kind have been presented by Jørgensen and co-workers within the context of the CCLR theory, addressing the size consistency of the CC excitation energies [8] and transition moments [19], and analyzing the truncation errors in the CC excitation energies [20, 21]. Studies devoted to the size consistency of the excited-state CC equations have also been presented by Mukhopadhyay et al. [22] and Stanton [23]. From a different perspective, the so-called order relations of the bCC secular matrix and the ensuing truncation errors in the CC excitation energies have been discussed by the present authors [18] and by Trofimov et al. [24]. However, the latter studies, devised essentially to enable comparison to the algebraic-diagrammatic construction (ADC) propagator methods [24–26], were somewhat limited and suffered, moreover, from certain misconceptions concerning the CC transition moments.

The analysis given in this paper of the excited-states CC approach will be formulated entirely within the framework of the bCC concept, that is, a non-hermitian secular problem associated with a dual representation of the (shifted) Hamiltonian in terms of two biorthogonal sets of basis states. While in the EOM-CC development, the bCC representation is introduced more or less in an ad hoc manner, depicting the bCC secular matrix essentially as a CI-type representation of an effective (similarity transformed) Hamiltonian, the CCLR approach is based on response theory for time-dependent CC ground-state expectation values. Clearly, the CCLR derivation is highly original and instructive, and, in fact, transcends the simple bCC formulation in the case of the transition moments and various reponse properties. However, the essence of the emerging computational scheme can much easier be presented and understood using the bCC concept. Thus, it should be permissible and even advisable to abandon the original notations associated with linear response theory and rather resort to a stringent wave function formulation adapted to the bCC concept. Not only will this make the excited-state CC methods more amenable to readers not familiar with the rather demanding time-dependent CC response theory, it will also allow us to embed the CC approach quite naturally in the broader context of ISR methods.

An outline of the paper is as follows. In Sect. 2, we briefly review the CI method with regard to the truncation error and separability properties. Section 3 presents the basics of the CC approach to electronic excitation. This is followed in Sect. 4 by an analysis of the properties of the bCC representation and the resulting excitation energies, transition moments and excited-state properties. Section 5 contrasts the bCC representation with a full (hermitian) ISR approach. A summary and some conclusions are given in the final Sect. 6. Some important supporting material is

presented in a tripartite Appendix. In Appendix 1 the proof of the bCC order relations is reviewed. In Appendix 2, we derive the order relations of both CI and bCC eigenvector matrices, which, in turn, allows us to generate general truncation error formulas. The CCLR forms of the right transition moments and excited-state properties are reviewed in Appendix 3.

2 A look at the CI method

The justification of the intrinsically more complicated intermediate state representations derives from basic shortcomings of the standard configuration-interaction (CI) approach with regard to the truncation error of the CI expansions and the size consistency of the results. To provide for a general background, we begin with a brief recapitulation of the CI problems.

For the electronically excited states $|\Psi_n\rangle$ of an atom or molecule, the Schrödinger equation may be written in the form

$$(\hat{H} - E_0)|\Psi_n\rangle = \omega_n|\Psi_n\rangle \tag{1}$$

where $\hat{H}$ is the Hamiltonian of the system under consideration, and E_0 and $\omega_n = E_n - E_0$ denote the ground-state energy and excitation energy, respectively. In the CI treatment, being the standard quantum chemical method, the excited states are expanded according to

$$|\Psi_n\rangle = \sum_J X_{Jn}|\Phi_J\rangle \tag{2}$$

as a linear combination of CI states

$$|\Phi_J\rangle = \hat{C}_J|\Phi_0\rangle \tag{3}$$

generated by applying "physical" excitation operators $\hat{C}_J$ to the HF ground state, $|\Phi_0\rangle$. Using the notation of second quantization, the excitation operator manifold may be expressed as follows:

$$\{\hat{C}_J\} \equiv \left\{c_a^\dagger c_k; c_a^\dagger c_b^\dagger c_k c_l, a<b, k<l; \ldots\right\} \tag{4}$$

Here $c_p^\dagger(c_p)$ denote creation (annihilition) operators associated with the HF orbitals $|\phi_p\rangle$. Following a widely adopted convention, the subscripts a, b, c, ... and i, j, k, ... denote unoccupied (virtual) and occupied orbitals, respectively, while the indices p, q, r, ... will be used in the general case. The capital indices I, J, ... are used as an abbreviation for strings of one-particle indices, e.g., $I \equiv (a\ b\ k\ l)$.

The excitation operators in (4) can be divided into classes of p–h (single), $2p$–$2h$ (double), ... excitations. For brevity, these classes will be numbered consecutively, that is, the class of μp–μh excitations is referred to as class μ. The class of a particular excitation J will be denoted by $[J]$. For example, $[J] = 2$ means J is a double excitation. The HF ground state $|\Phi_0\rangle$, being part of the CI expansions (2), constitutes a zeroth class ($\mu = 0$).

The excitation energies and expansion coefficients are obtained as the eigenvalues and eigenvector components, respectively, of the CI eigenvalue problem, reading in a compact matrix notation

$$\boldsymbol{HX} = \boldsymbol{X\Omega}, \quad \mathbf{X}^\dagger\boldsymbol{X} = \mathbf{1} \tag{5}$$

Here $\boldsymbol{H}$ is the (subtracted) CI secular matrix,

$$H_{IJ} = \langle\Phi_I|\hat{H} - E_0|\Phi_J\rangle \tag{6}$$

$\boldsymbol{\Omega}$ denotes the diagonal matrix of excitation energies ω_n, and $\boldsymbol{X}$ is the matrix of (column) eigenvectors $\underline{X}_n$. Note that the subtraction of the ground-state energy E_0 in the diagonal of the CI secular matrix is a mere convention here, introduced for formal analogy to the bCC representation considered in Sect. 3.

Approximate CI treatments are obtained by limited CI expansions as opposed to full (FCI) expansions. In the following, we will be concerned with systematic truncations of the CI expansions, that is, expansions being complete through a given excitation class μ. These systematic truncation schemes can be examined with respect to the perturbation-theoretical (PT) order of the induced error in the CI results. For this purpose, one has to inspect the "order structure" of the CI secular matrix (Fig. 1), that is, a PT classification of the sub-blocks $\boldsymbol{H}_{\mu\nu}$ associated with a partitioning of $\boldsymbol{H}$ with respect to the excitation classes. Figure 1 shows the characteristic CI structure, where each excitation class is coupled linearly in the Coulomb

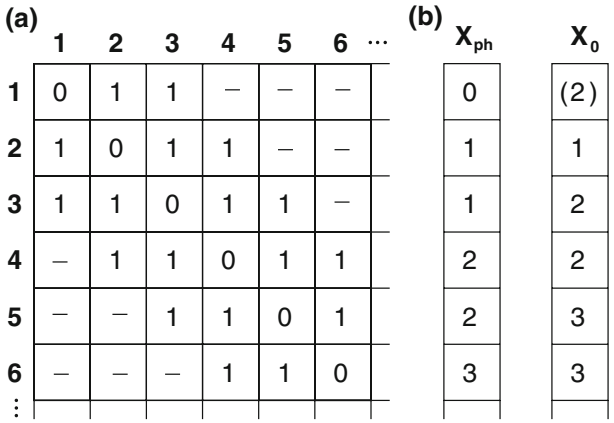

Fig. 1 **a** Order structure of the CI secular matrix $\boldsymbol{H}$. The sub-blocks correspond to the partitioning with respect to excitation classes of μp–μh (μ-particle–μ-hole) excitations, $\mu = 1, 2, \ldots$. The entries 0, 1 indicate the "PT order" of the blocks, being here simply 0 (in the diagonal blocks) or 1 (linear in the electron repulsion integrals); vanishing blocks are indicated by *dashes*. **b** Order relations of CI eigenvectors associated with singly excited states ($\boldsymbol{X}_{ph}$) and the ground state ($\boldsymbol{X}_0$). The entries denote the (lowest) PT order of the respective eigenvector segments

integrals (first order) to the next and next but one excitation class. Owing to the (zeroth order) orbital energy contributions of the diagonal matrix elements, the diagonal blocks are indicated by zeros.

The order structure of the CI secular matrix gives rise to characteristic truncation errors in the excitation energies. As the most important case, let us consider singly excited states, that is, states deriving perturbation-theoretically from p–h configurations (CI basis states). Due to the linear (first-order) coupling to triple ($3p$–$3h$) excitations (see Fig. 1), there is a second-order energy contribution to the single excitation energies arising from the admixture of triple excitations. This means that a second-order truncation error arises in the single-excitation energies if the triple excitations are not taken into account. A stringent derivation of the general CI truncation errors is given in Appendix 2 (CI eigenvector matrix). Specifically, the truncation error orders (TEO) for single excitation energies are given by the following formula:

$$O_{\mathrm{TE}}(\mu) = \begin{cases} \mu, & \mu \text{ even} \\ \mu + 1, & \mu \text{ odd} \end{cases} \tag{7}$$

Here μ denotes the highest excitation class included in the CI expansion manifold. In Table 1 the resulting TEOs for $\mu = 1, \ldots, 6$ are listed.

Besides the energies, the transition moments

$$T_n = \langle \Psi_n | \hat{D} | \Psi_0 \rangle \tag{8}$$

are of interest, being required to compute spectral intensities. Here $\hat{D}$ denotes a (one-particle) transition operator, e.g., a dipole operator component. To evaluate the truncation error of the transition moments, one has to analyze the CI expression

$$T_n = \underline{X}_n^{\dagger} \mathbf{D} \underline{X}_0 \tag{9}$$

with respect to the order relations of the CI eigenvectors $\underline{X}_n$ and $\underline{X}_0$, respectively, and the CI representation of $\hat{D}$,

Table 1 Truncation errors (PT order) for excitation energies, transition moments and excited-state properties of singly excited states

Truncation level	Excitation energies			Transition moments			Properties		
	CI	bCC	ADC	CI	bCC	ADC	CI	bCC	ADC
1	2	2	2	1	1	2	1	1	1
2	2	3	4	2	3	4	2	2	3
3	4	5	6	3	4	6	3	4	5
4	4	6	8	4	6	8	4	5	7
5	6	8	10	5	7	10	5	7	9
6	6	9	12	6	9	12	6	8	11

Comparison of CI, bCC and ADC approaches at the lowest six truncation levels

$$D_{IJ} = \langle \Phi_I | \hat{D} | \Phi_J \rangle. \tag{10}$$

The order relations of the CI eigenvectors for singly excited states and for the ground state, shown in Fig. 1, are part of the general order structure of the CI eigenvector matrix $\boldsymbol{X}$, derived in Appendix 2 (CI eigenvector matrix). Together with the trivial order structure of $\boldsymbol{D}$ (zeroth-order diagonal and off-diagonal blocks, other matrix elements vanishing), one can deduce the following simple TEO expression for the transition moments of singly excited states:

$$O_{\mathrm{TE}}(\mu) = \mu \tag{11}$$

For odd values of μ, the TEOs of the transition moments are smaller by 1 as compared to the excitation energies.

The CI truncation errors are relatively large, which, in turn, implies that large CI expansions are required to meet specific accuracy levels. For example, in order to treat singly excited states consistently through second order of PT, the CI configuration space must comprise the triple excitations ($\mu = 3$). By contrast, in the ISR methods, a much smaller explicit configuration space, consisting of single and double excitations, affords the corresponding level of accuracy.

To analyze the size-consistency properties of a method, one usually resorts to the separate fragment model, that is, a system S consisting of two strictly non-interacting fragments, A and B. A method for treating electronic excitation is size consistent (here, more specifically, size intensive) if for local excitations, say on fragment A, the computed excitation energies and transition moments do not depend on whether the method is applied to the fragment or to the composite system. It is well known that truncated CI treatments do not fulfill this property. There is an uncontrollable size-consistency error in the treatment of the total system, corrupting not only the results for the separate fragment model, but, more generally, any truncated CI treatment of larger molecules. This can be nicely demonstrated in the exactly solvable model of a chain of non-interacting two-electron two-orbital ($2E$–$2O$) systems, such as $1s^2 2s^0$ He atoms or minimal basis H_2 molecules (see, for example, Meunier and Levy [27]). Because of this deficiency, the CI method does not qualify as a genuine many-body method.

As a preparation for the analysis of the bCC schemes, let us briefly inspect the case of CI in some more detail. Obviously, the Hamiltonian for S decomposes into the sum of the fragment Hamiltonians, $\hat{H} = \hat{H}_A + \hat{H}_B$. Moreover, the one-particle states (HF orbitals) of S can be classified as belonging either to fragment A or B (local on A or B, respectively). Accordingly, the CI states can be partitioned into three different sets, that is, local excitations I_A on fragment A, local excitations I_B on fragment B, and mixed (or non-local) excitations I_{AB} involving both fragment A

and B. In the latter class, we may disregard any excitations that do not conserve the local electron number, e.g., A^+B^- charge-transfer excitations. In the non-interacting fragment model, such charge transfer excitations are strictly decoupled from the fragment-charge conserving excitations, which are of interest here.

The CI configurations $|\Phi_I\rangle$ can be written as products of fragment states, e.g.,

$$\begin{aligned} |\Phi_0\rangle &= |\Phi_0^A\rangle|\Phi_0^B\rangle \\ |\Phi_{I_A}\rangle &= |\Phi_{I_A}^A\rangle|\Phi_0^B\rangle \\ |\Phi_{I_AI_B}\rangle &= |\Phi_{I_A}^A\rangle|\Phi_{I_B}^B\rangle \end{aligned} \tag{12}$$

It should be noted that the neglect of full antisymmetrization of these product states is irrelevant, because in the non-interacting fragment model, matrix elements are not affected by inter-fragment antisymmetrization. Figure 2 shows the partitioning of the CI secular matrix with respect to the three different types of configurations, that is, local excitations on fragment A, local excitations on fragment B and non-local excitations, respectively. While the A and B states are strictly decoupled, $\boldsymbol{H}_{AB} = \mathbf{0}$, there is a coupling between the local and mixed excitations, e.g.,

$$H_{I_A,J_AJ_B} = \delta_{I_AJ_A}\langle\Phi_0^B|\hat{H}_B|\Phi_{J_B}^B\rangle \tag{13}$$

as can easily be derived using the CI state factorization according to Eq. 12. An explicit example is the coupling matrix element

$$H_{ak,bc'd'i'j'l} = \delta_{ab}\delta_{kl}V_{c'd'[i'j']} \tag{14}$$

for a single excitation $I_A = (ak)$ associated with fragment A and a non-local triple excitation $J_{AB} = (bl,c'd'i'j')$. Here, the unprimed (primed) indices denote fragment A (fragment B) one-particle states; $V_{pq[rs]}$ denotes the anti-symmetrized Coulomb integral.

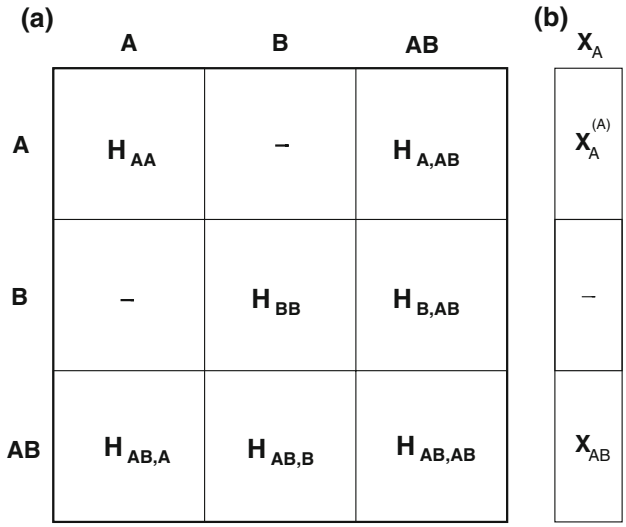

Fig. 2 **a** Block structure of the CI secular matrix $\boldsymbol{H}$ corresponding to the partitioning associated with the separate fragment model (see text). **b** Structure of CI eigenvectors for a local excitation (on fragment A)

Given the structure as shown in Fig. 2, the CI secular matrix is said to be *non-separable* because there is no a priori decoupling of local excitations (say on fragment A) from non-local (or mixed) excitations. The CI treatment of the composite system S aims in an inextricable way at an optimal description of both fragments, that is, the excited state of fragment A and the ground state of fragment B. In the exact (full) CI result, say for the energy $E_n = E_n^A + E_0^B$ of the locally excited system, the ground-state energy E_0^B of the unaffected fragment B would cancel exactly upon subtraction of the exact ground-state energy $E_0 = E_n^A + E_0^B$ of S, so that, of course, the full CI excitation energy, $E_n - E_0 = E_n^A - E_0^A$, is size consistent. At the level of a limited CI expansion, however, neither the excited-state energy nor the ground-state energy are simply the sums of the fragment energies.

3 Biorthogonal CC representation

The bCC formulation (see, for example, Helgaker et al. [28]) is based on a mixed representation of the (subtracted) Hamiltonian, $\hat{H} - E_0$, in terms of two sets of left and right expansion manifolds: (1) the CC states

$$\left|\Psi_J^0\right\rangle = \hat{C}_J\left|\Psi_0^{\mathrm{cc}}\right\rangle = \hat{C}_J e^{\hat{T}}|\Phi_0\rangle \tag{15}$$

on the right-hand side, and (2) the associated biorthogonal states

$$\left\langle\overline{\Phi}_I\right| = \langle\Phi_0|\hat{C}_I^\dagger e^{-\hat{T}} \tag{16}$$

on the left-hand side. Here $\hat{C}_I$ denotes the physical excitation operator as specified in Eq. 4. The familiar ground-state CC parametrization (and normalization)

$$\left|\Psi_0^{\mathrm{cc}}\right\rangle = e^{\hat{T}}|\Phi_0\rangle \tag{17}$$

is used, where $|\Phi_0\rangle$ denotes the HF ground state, and

$$\hat{T} = \sum_I t_I\hat{C}_I \tag{18}$$

is the cluster operator with the amplitudes t_J determined by the ground-state CC equations. The $\hat{T}$ operator, comprising physical excitation operators only, commutes with any (physical) $\hat{C}_J$ operator, so that the CC states of Eq. 15 can likewise be written as

$$\left|\Psi_J^0\right\rangle = e^{\hat{T}}\hat{C}_J|\Phi_0\rangle \tag{19}$$

The biorthonormality of the two sets of states,

$$\left\langle\overline{\Phi}_I|\Psi_J^0\right\rangle = \langle\Phi_I|e^{-\hat{T}}e^{\hat{T}}|\Phi_J\rangle = \delta_{IJ} \tag{20}$$

is an obvious consequence of the orthonormalization of the CI configurations $|\Phi_J\rangle = \hat{C}_J|\Phi_0\rangle$.

The bCC representation of $\hat{H} - E_0$ gives rise to a non-hermitian secular matrix $\mathbf{M}$ with the elements

$$M_{IJ} = \langle \overline{\Phi}_I | \hat{H} - E_0 | \Psi_J^0 \rangle = \langle \Phi_0 | \hat{C}_I^\dagger e^{-\hat{T}} [\hat{H}, \hat{C}_J] e^{\hat{T}} | \Phi_0 \rangle \quad (21)$$

In the latter form, the (CC) ground-state energy E_0 no longer appears explicitly. Let us note that the bCC secular matrix can also be written as a CI representation

$$M_{IJ} = \langle \Phi_I | \overline{H} - E_0 | \Phi_J \rangle$$

of the similarity transformed Hamiltonian, $\overline{H} = e^{-\hat{T}} \hat{H} e^{\hat{T}}$. However, this form is less transparent than the bCC representation (21) and, thus, less useful for the analysis intended here.

The (vertical) electronic excitation energies, $\omega_n = E_n - E_0$, can be identified as the eigenvalues of the CC secular matrix $\mathbf{M}$. Because $\mathbf{M}$ is not hermitian, one has to deal with right and left eigenvalue problems,

$$\mathbf{MX} = \mathbf{X\Omega} \quad (22)$$

$$\mathbf{Y}^\dagger \mathbf{M} = \mathbf{\Omega Y}^\dagger \quad (23)$$

where $\mathbf{\Omega}$ is the diagonal matrix of eigenvalues ω_n, and $\mathbf{X}$ and $\mathbf{Y}$ denote the matrices of the right and left eigenvectors, respectively. To obtain a definite normalization, the two sets of secular equations have to be combined according to

$$\mathbf{Y}^\dagger \mathbf{MX} = \Omega, \quad \mathbf{Y}^\dagger \mathbf{X} = 1 \quad (24)$$

so that the resulting right and left eigenvectors form two mutually biorthonormal sets. As a consequence, the corresponding right and left excited states,

$$|\Psi_n^{\rm cc}\rangle = \sum_I X_{In} |\Psi_I^0\rangle \quad (25)$$

$$\langle \Psi_m^{(l)}| = \sum_I Y_{Im}^* \langle \overline{\Phi}_I| \quad (26)$$

are biorthonormal too, $\langle \Psi_m^{(l)} | \Psi_n^{\rm cc} \rangle = \delta_{mn}$.

In general, the right excited states $|\Psi_n^{\rm cc}\rangle$ are not yet eigenstates of $\hat{H}$, because the underlying $|\Psi_I^0\rangle$ expansion manifold of Eq. 15 is incomplete as long as the CC ground state $|\Psi_0^{\rm cc}\rangle$ is not taken into account. Using the extended CC expansion manifold $\{R\} = \{|\Psi_0^{\rm cc}\rangle, |\Psi_I^0\rangle\}$ on the right-hand side, and, likewise, the extended biorthogonal manifold $\{L\} = \{\langle \Phi_0|, \langle \overline{\Phi}_I|\}$ on the left side, one arrives at the full bCC representation of $\hat{H} - E_0$ associated with the extended secular matrix

$$\mathbf{M}' = \begin{pmatrix} 0 & \underline{v}^{\rm t} \\ \underline{0} & \mathbf{M} \end{pmatrix} \quad (27)$$

Here $\underline{v}^{\rm t}$ is a transposed (row) vector with the elements

$$v_I = \langle \Phi_0 | \hat{H} | \Psi_I^0 \rangle \quad (28)$$

that is, the coupling matrix elements between the HF ground state and the excited CC states. Let us note that in the usage of the EOM-CC approach, $\mathbf{M}'$ is denoted by $\overline{\mathbf{H}}$. In the CCLR context, on the other hand, the (inner) bCC secular matrix $\mathbf{M}$ (Eq. 21) is referred to as the CC Jacobian $\mathbf{A}$ and the coupling vector $\underline{v}^{\rm t}$ is denoted by $\boldsymbol{\eta}$.

The two expansion manifolds used in the bCC representation are of quite different quality. The "correlated excited states" (CES) of the set $\{R\}$ are superior to the biorthogonal $\{L\}$ states, if more complex. Obviously, a CC state of class $[I]$ can be written according to

$$|\Psi_I^0\rangle = e^{\hat{T}} |\Phi_I\rangle = |\Phi_I\rangle + \sum_{K,[K]>[I]} z_K^{(I)} |\Phi_K\rangle \quad (29)$$

as a linear combination of $|\Phi_I\rangle$ and CI configurations of *higher* excitation classes, $[K] > [I]$, extending through N-tuple excitations. By contrast, the CI expansion of a biorthogonal $\{L\}$ set state reads

$$\langle \overline{\Phi}_I| = \langle \Phi_I | e^{-\hat{T}} = \langle \Phi_I| + \sum_{K,[K]<[I]} z_K^{(I)} \langle \Phi_K| \quad (30)$$

that is, a linear combination of $\langle \Phi_I|$ and *lower* class CI excitations, $[K] < [I]$, including the zeroth class, $[K] = 0$. This follows from the observation that $z_K^{(I)} = \langle \Phi_I | e^{-\hat{T}} | \Phi_K \rangle$ vanishes for $[K] > [I]$ (and $z_K^{(I)} = \delta_{IK}$ for $[K] = [I]$).

As is easily seen, the linear space spanned by the biorthogonal states through a given excitation class μ is identical with the corresponding space of CI configurations:

$$\text{span}\{\langle \Phi_I | e^{-\hat{T}}, [I] = 0, 1, \ldots, \mu\} = \text{span}\{\langle \Phi_I |, [I] = 0, 1, \ldots, \mu\} \quad (31)$$

This means that (truncated) expansions in terms of the biorthogonal ($\{L\}$ set) states are essentially of the CI type. Let us note that the SAC-CI equations are obtained by using the CI expansion manifold for the left eigenstates rather than the $\{L\}$ states [15–17].

As will be discussed below, the use of a CI-type expansion manifold on the left-hand side of the bCC representation deteriorates the overall order relations and separability properties to a certain extent. One may wonder then why one could not simply use the CC states as the common expansion manifold for both sides of the secular matrix. However, in such an approach, referred to as variational or unitary CC version (see Kutzelnigg [29] and Szalay et al. [30]), there is a major problem associated with evaluating the secular (and overlap) matrix elements: being of the form $\langle \Phi_I | e^{\hat{T}^\dagger} \hat{H} e^{\hat{T}} | \Phi_J \rangle$, there is no obvious truncation of higher excitation contributions (below N-tuple excitation level).

Let us now briefly inspect the eigenpair manifold of the extended bCC secular matrix $\mathbf{M}'$. Obviously, there is one more eigenvalue, $\omega_0 = 0$, corresponding to the ground state, while the excited-state eigenvalues, ω_n, $n > 0$, of the sub-block $\mathbf{M}$ are also eigenvalues of $\mathbf{M}'$. The corresponding extended left and right eigenvectors can easily be

determined. Let us first consider the ground-state solutions. Here the right eigenvector is trivial,

$$\underline{X}_0 = \begin{pmatrix} 1 \\ \underline{0} \end{pmatrix} \tag{32}$$

which is consistent with the fact that $\left|\Psi_0^{\mathrm{cc}}\right\rangle$ is the exact ground state. Less obvious is the left ground-state eigenvector

$$\underline{Y}_0'^{\dagger} = \left(1, \underline{Y}_0^{\dagger}\right) \tag{33}$$

where the row vector $\underline{Y}_0^{\dagger}$ can explicitly be obtained from $\mathbf{M}$ and $\underline{v}$ according to

$$\underline{Y}_0^{\dagger} = -\underline{v}^{\mathrm{t}}\mathbf{M}^{-1} \tag{34}$$

The corresponding representation of the ground state,

$$\langle\overline{\Psi}_0| = \langle\Phi_0| + \sum_I Y_{I0}^{*}\langle\overline{\Phi}_I| \tag{35}$$

in terms of the biorthogonal bCC states is referred to as the "dual" ground state [7]. In the CCLR nomenclature, the dual ground state is denoted by $\langle\Lambda|$. As will be discussed below, the dual ground state is a non-separable CI-type representation of the ground state, leading to undesired features in the bCC transition moments.

The left excited-state eigenvectors of $\mathbf{M}'$ are obtained as obvious extensions according to

$$\underline{Y}_n'^{\dagger} = (0, \underline{Y}_n^{\dagger}) \tag{36}$$

from the left eigenvectors of the $\mathbf{M}$ sub-block. This means that the excited states $\langle\Psi_n^{(l)}|$ of Eq. 26 are proper eigenstates of $\hat{H}$. In particular, they are orthogonal to the exact CC ground state,

$$\left\langle\Psi_n^{(l)}|\Psi_0^{\mathrm{cc}}\right\rangle = 0 \tag{37}$$

which follows from $\left\langle\overline{\Phi}_I|\Psi_0^{\mathrm{cc}}\right\rangle = 0$.

In general, that is, if not forbidden by symmetry, the right extended eigenvectors acquire non-vanishing zeroth components $x_n = X_{n0}'$, and the extended eigenvectors take on the form

$$\underline{X}_n' = \begin{pmatrix} x_n \\ \underline{X}_n \end{pmatrix} \tag{38}$$

where $\underline{X}_n$ is the (nth) eigenvector of the $\mathbf{M}$ sub-block, and the zeroth component x_n is given by

$$x_n = \omega_n^{-1}\underline{v}^{\mathrm{t}}\underline{X}_n \tag{39}$$

Since $\mathbf{M}\underline{X}_n = \omega_n\underline{X}_n$, the following relations hold:

$$x_n = \underline{v}^{\mathrm{t}}\mathbf{M}^{-1}\underline{X}_n = -\underline{Y}_0^{\dagger}\underline{X}_n \tag{40}$$

Here Eq. 34 has been used to arrive at the last expression.

As a consequence, the right expansion of an excited eigenstate takes on the form

$$|\Psi_n^{(r)}\rangle = x_n|\Psi_0^{\mathrm{cc}}\rangle + |\Psi_n^{\mathrm{cc}}\rangle \tag{41}$$

where $\left|\Psi_n^{\mathrm{cc}}\right\rangle$ is given by Eq. 25. Let us note that $\langle\Phi_0|\Psi_n^{\mathrm{cc}}\rangle = 0$, since $\langle\Phi_0|\Psi_I^0\rangle = 0$, so that the relation

$$x_n = \langle\Phi_0|\Psi_n^{(r)}\rangle \tag{42}$$

can be established. The excited eigenstates $|\Psi_n^{(r)}\rangle$ are manifestly orthogonal to the dual ground state:

$$\langle\overline{\Psi}_0|\Psi_n^{(r)}\rangle = x_n + \underline{Y}_0^{\dagger}\underline{X}_n = 0 \tag{43}$$

where the relations $\langle\overline{\Phi}_I|\Psi_n^{(r)}\rangle = X_{In}$ and Eq. 40 have been used.

For spectral intensities, the squared moduli $|T_n|^2$ of the transition moments (8) are required, involving normalized ground and excited states. In the bCC representation a properly normalized expression for $|T_n|^2$ is obtained according to [14, 19]

$$|T_n|^2 = \langle\overline{\Psi}_0|\hat{D}|\Psi_n^{(r)}\rangle\langle\Psi_n^{(l)}|\hat{D}\left|\Psi_0^{\mathrm{cc}}\right\rangle \tag{44}$$

using both the left and right transition moments,

$$T_n^{(l)} = \langle\Psi_n^{(l)}|\hat{D}|\Psi_0^{\mathrm{cc}}\rangle \tag{45}$$

$$T_n^{(r)} = \langle\overline{\Psi}_0|\hat{D}|\Psi_n^{(r)}\rangle \tag{46}$$

Individually, the left and right transition moments have no significance because the respective ground and excited states are not normalized. However, the biorthonormality relations $\left\langle\overline{\Psi}_0|\Psi_0^{\mathrm{cc}}\right\rangle = \langle\Psi_n^{(l)}|\Psi_n^{(r)}\rangle = 1$ ensure the combined normalization in the product (44). In contrast to the left transition moments, the ordinary bCC form (46) for the right transition moments is not separable, so that the results obtained at truncated bCC levels are not size intensive [19]. Within the CCLR framework, this shortcoming is avoided, as here a separable, if a more elaborate expression, is employed for the right transition moments [7, 19]. The different treatment of the spectral intensities is a distinguishing feature of the otherwise equivalent CCLR and EOM–CC methods. In Sect. 4.4 and Appendix 3, the CCLR expression for the right transition moments will briefly be reviewed.

As will be discussed, the problem in the right transition moments does not result from the right eigenstates, but rather from the use of the dual ground state $\left\langle\overline{\Psi}_0\right|$. As can be concluded from Eqs. 30, 34 and 35, the dual ground state is a CI-type expansion of the form

$$\left\langle\overline{\Psi}_0\right| = \langle\Phi_0| + \sum_{K>0}\tilde{z}_K\langle\Phi_K| \tag{47}$$

where the expansion coefficients depend (via Eqs. 34, 35) on the t-amplitudes of the CC ground state. For the CC ground-state energy, the following relation holds:

$$E_0^{\rm cc} = \langle \overline{\Psi}_0 | \hat{H} | \Psi_0^{\rm cc} \rangle \tag{48}$$

It should be noted that this expression applies not only to the exact CC ground state (where $E_0^{\rm cc} = E_0$), but also to CC approximations based on truncations of the expansion manifolds, such as in CCSD. This can be seen by writing the RHS of Eq. 48 more explicitly as

$$\langle \overline{\Psi}_0 | \hat{H} | \Psi_0^{\rm cc} \rangle = \langle \Phi_0 | \hat{H} | \Psi_0^{\rm cc} \rangle + \sum_I Y_{I0}^* \langle \overline{\Phi}_I | \hat{H} | \Psi_0^{\rm cc} \rangle \tag{49}$$

The first term on the RHS is the CC energy equation, while the second (summation) term vanishes in compliance with the CC amplitude equations, $\langle \overline{\Phi}_I | \hat{H} | \Psi_0^{\rm cc} \rangle = \langle \Phi_I | e^{-\hat{T}} \hat{H} e^{\hat{T}} | \Phi_0 \rangle = 0$.

What is the relation of the dual ground state to the CI ground state in the case of truncated expansions? Obviously, the energy expectation value of the dual ground state will always be greater than (or equal to) the corresponding CI energy,

$$\frac{\langle \overline{\Psi}_0 | \hat{H} | \overline{\Psi}_0 \rangle}{\langle \overline{\Psi}_0 | \overline{\Psi}_0 \rangle} \geq E_0^{\rm CI} \tag{50}$$

because the dual state expansion coefficients are non-variational. This can be well demonstrated in the exactly solvable model of 2 (or more) non-interacting $2E$–$2O$ systems (He atoms, or H_2 molecules).

It should be noted that the right and left eigenvalue problems (22, 23) for the secular matrix $\mathbf{M}$ (Eq. 21) follow from a variational principle, $\delta \langle \overline{\Phi} | \hat{H} | \Psi \rangle = 0$. under the constraint $\langle \overline{\Phi} | \Psi \rangle = 1$. Independent variations $\langle \delta \overline{\Phi} |$ and $| \delta \Psi \rangle$ on the left and right side of the energy and overlap matrix elements lead directly to the right and left eigenvalue equations, respectively.

4 Analysis of bCC excitation energies and intensities

4.1 Order relations and separability of the bCC secular matrix

Figure 3 shows the order structure of the bCC secular matrix $\mathbf{M}$. For the partitioning according to excitation classes, $\mu = 1, 2, \ldots$, the lowest (non-vanishing) PT orders are given here in the respective $\mathbf{M}_{\mu\nu}$ sub-blocks. In the upper right (UR) triangular part, we recover the characteristic CI structure of Fig. 1. This outcome can readily be understood by inspecting the general expression for the secular matrix elements,

$$\langle \overline{\Phi}_I | \hat{H} | \Psi_J^0 \rangle = \langle \Phi_I | \hat{H} | \Phi_J \rangle + \sum_{[K]<[I]} \sum_{[L]>[J]} z_K^{(I)} z_L^{(J)} \langle \Phi_K | \hat{H} | \Phi_L \rangle \tag{51}$$

(a)

	1	2	3	4	5	6	⋯
1	0	1	1	–	–	–	
2	1	0	1	1	–	–	
3	2	1	0	1	1	–	
4	3	2	1	0	1	1	
5	4	3	2	1	0	1	
6	5	4	3	2	1	0	
⋮							

(b)

	X_{ph}	Y_{ph}	Y_0
1	0	0	(2)
2	1	1	1
3	2	1	2
4	3	2	2
5	4	2	3
6	5	3	3
⋮			

Fig. 3 **a** Order relations of the bCC secular matrix $\boldsymbol{M}$. As in Fig. 1, the block structure reflects the partitioning of $\boldsymbol{M}$ with respect to excitation classes $\mu = 1, 2, \ldots$, The entries denote the (lowest) PT order of the matrix elements in the respective sub-block; vanishing blocks are indicated by *dashes*. **b** Order relations of bCC eigenvectors: $\boldsymbol{X}_{ph}$ and $\boldsymbol{Y}_{ph}$ denote right and left eigenvectors for singly excited states; $\boldsymbol{Y}_0$ is the "dual" CC ground state

obtained by using the expansions (29, 30) for the CC and biorthogonal states, respectively. For the UR matrix elements with $[I] < [J]$, the sums on the RHS of Eq. 51 do not contribute, because the excitation classes of the double summation indices K and L differ at least by a triple excitation, $[L] - [K] \geq 3$, so that the Hamiltonian matrix elements $\langle \Phi_K | \hat{H} | \Phi_L \rangle$ vanish. This means that the bCC and CI secular matrix elements are identical, $M_{IJ} = H_{IJ}$, for $[I] < [J]$. For the diagonal blocks $\mathbf{M}_{\mu\mu}$, of course, the lowest non-vanishing PT order is zero because the perturbation expansions of the diagonal matrix elements M_{II} begin with zeroth-order (HF) excitation energies.

By contrast, the lower left (LL) triangular part, $[I] \geq [J]$, gives rise to the remarkable "canonical" order relations, reading

$$M_{IJ} \sim O([I] - [J]), \quad [I] \geq [J] \tag{52}$$

This means that the lowest non-vanishing contribution in the PT expansion of the matrix element M_{IJ}, $[I] \geq [J]$ is of the order $[I] - [J]$. Likewise, we will use the notation $O[M_{IJ}] = [I] - [J]$. These order relations were first specified by Christiansen et al. [31], quite explicitly, for the lowest five excitation classes (singles through pentuples) and later by Hald et al. [21] for general levels of excitation. A first general proof of the bCC order relations was given in Ref. [18]. A brief recapitulation of this proof is given in Appendix 1.

It should be noted that these canonical order relations are highly non-trivial, indeed. Let us consider, for example, the $\boldsymbol{M}_{31}$ matrix elements, being of the order 2. This means that the apparent first-order contribution arising from the leading (CI) term on the RHS of Eq. 51 is exactly cancelled by other first-order contributions from the summation part.

The bCC order structure gives rise to specific truncation errors of the excitation energies, which can be analyzed by

inspecting formal PT interaction paths on the sub-blocks of the bCC secular matrix. As an example, let us consider the following path:

$$M_{11}(0) \rightarrow M_{13}(1) \rightarrow M_{33}(0) \rightarrow M_{31}(2) \rightarrow M_{11}(0)$$

This path allows one to specify formally a PT contribution in the excitation energy of a single excitation (class 1) arising from the admixture of triple excitations (class 3). The PT order of this path is 3, and there is no lower-order path involving class 3. This means that the PT contributions to single excitation energies arising from triple excitations are of the order 3. Stated differently, the truncation error for single excitation energies due to the neglect of triple excitations in the explicit bCC expansion manifold is of third order, as compared to a second-order truncation error in the CI treatment.

A more general and stringent derivation of the bCC truncation errors is to be based on the order relations of the bCC eigenvector matrices, as discussed in Appedix 2. In short, the order relations in the bCC secular matrix induce corresponding order relations for the left and right eigenvector matrices $\boldsymbol{Y}$ and $\boldsymbol{X}$, respectively. As shown in Fig. 10, the bCC eigenvector matrices combine canonical and CI-type behavior: the LL part of $\boldsymbol{X}$ and the UR part of $\boldsymbol{Y}$ exhibit canonical order relations, whereas CI-type order relations (Fig. 9) apply to the UR part of $\boldsymbol{X}$ and the LL part of $\boldsymbol{Y}$. The eigenvector order relations, in turn, allow one to analyze the truncation errors in the excitation energies, transition moments and excited-state properties. For the singly excited states, the TEO in the bCC excitation energies are given by the following formula (deriving from Eq. 185)

$$O_{\mathrm{TE}}(\mu) = \begin{cases} \frac{3}{2}\mu, & \mu \text{ even} \\ \frac{3}{2}\mu + \frac{1}{2}, & \mu \text{ odd} \end{cases} \tag{53}$$

Here μ denotes the highest excitation class in the expansion manifold. In Table 1, the TEOs in the excitation energies of singly excited states are listed for the first six truncation levels.

To discuss the *separability properties* of the bCC schemes [8, 19, 28] (see also Refs. [22, 23]) we revisit the separate fragment model, $S \equiv A + B$, considered in Sect. 2. Like the Hamiltonian, $\hat{H} = \hat{H}_A + \hat{H}_B$, also the CC operator can be written as the sum of the fragment operators, $\hat{T} = \hat{T}_A + \hat{T}_B$. As a consequence, both the CC states $\left|\Psi_I^0\right\rangle$ and the biorthogonal states $\left\langle\overline{\Phi}_I\right|$ used in the right and left expansion manifolds, respectively, can be written as products of fragment A and B states:

$$\begin{aligned} \left|\Psi_{I_A}^0\right\rangle &= \left|\Psi_{I_A}^A\right\rangle\left|\Psi_0^B\right\rangle, \ \left|\Psi_{I_AI_B}^0\right\rangle = \left|\Psi_{I_A}^A\right\rangle\left|\Psi_{I_B}^B\right\rangle \\ \left\langle\overline{\Phi}_{I_A}\right| &= \langle\overline{\Phi}_{I_A}^A|\langle\Phi_0^B|, \langle\overline{\Phi}_{I_AI_B}| = \langle\overline{\Phi}_{I_A}^A|\langle\overline{\Phi}_{I_B}^B| \end{aligned} \tag{54}$$

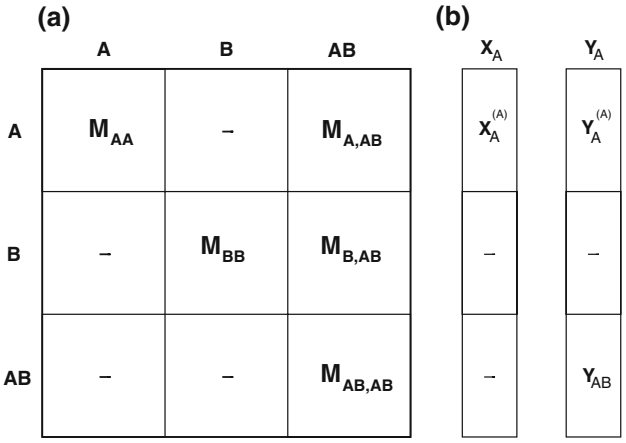

Fig. 4 **a** Block structure of the bCC secular matrix $\boldsymbol{M}$ corresponding to the partitioning associated with the separate fragment model (see text). **b** Structure of right and left bCC eigenvectors for a local excitation (on fragment A)

Here, the notation of the fragment states has been somewhat simplified by omitting the superscripts 0 and cc: for example, $\left|\Psi_{I_A}^A\right\rangle \equiv \left|\Psi_{I_A}^{A,0}\right\rangle$ and $\left|\Psi_0^B\right\rangle \equiv |\Psi_0^{B,\mathrm{cc}}\rangle$. Figure 4 shows the partitioning of the bCC secular matrix with respect to the three different types of configurations, that is, local excitations on fragment A, local excitations on fragment B and non-local (or mixed) excitations. Let us note once again that in the latter set we can disregard any charge-transfer type of configurations.

The separability properties of the bCC secular matrix, as shown in Fig. 4, can be readily derived by using the factorization (Eq. 54) of the bCC basis functions. As an explicit example, let us derive that the block $\boldsymbol{M}_{AB,A}$ vanishes:

$$\begin{aligned} M_{I_AI_B,J_A} &= \langle\overline{\Phi}_{I_AI_B}|\hat{H}_A + \hat{H}_B|\Psi_{J_A}^0\rangle \\ &= \langle\overline{\Phi}_{I_A}^A|\hat{H}_A|\Psi_{J_A}^A\rangle\langle\overline{\Phi}_{I_B}^B|\Psi_0^B\rangle + \langle\overline{\Phi}_{I_A}^A|\Psi_{J_A}^A\rangle\langle\overline{\Phi}_{I_B}^B|\hat{H}_B|\Psi_0^B\rangle = 0 \end{aligned} \tag{55}$$

Here, the first term on the RHS vanishes because of the orthogonality relation $\langle\overline{\Phi}_{I_B}^B|\Psi_0^B\rangle = 0$. The second term vanishes,

$$\langle\overline{\Phi}_{I_B}^B|\hat{H}_B|\Psi_0^B\rangle = E_0^B\langle\overline{\Phi}_{I_B}^B|\Psi_0^B\rangle = 0 \tag{56}$$

because $|\Psi_0^B\rangle$ is an eigenfunction of $\hat{H}_B$, and $\langle\overline{\Phi}_{I_B}^B|$ and $|\Psi_0^B\rangle$ are orthogonal. In fact, this result is not predicated on the exact fragment B ground state, but applies also to any (systematic) CC approximation, since $\langle\overline{\Phi}_{I_B}^B|\hat{H}_B|\Psi_0^B\rangle = 0$ is satisfied as CC amplitudes equation for fragment B.

In a similar way, one may establish that the bCC secular matrix for fragment A is identical to the (A, A)-block of the composite system secular matrix,

$$\boldsymbol{M}_{AA} = \boldsymbol{M}^A \tag{57}$$

In deriving this result, one utilizes the CC equation for the ground state of fragment B, $\langle\Phi_0^B|\hat{H}_B - E_0^B|\Psi_0^B\rangle = 0$. The matrix elements in the non-vanishing (A, AB) coupling block read

$$M_{I_A,J_AJ_B} = \delta_{I_AJ_A} v_{J_B}^B \tag{58}$$

where $v_{J_B}^B = \langle\Phi_0^B|\hat{H}_B|\Psi_{J_B}^B\rangle$. Finally, the non-local diagonal block matrix elements are given by

$$M_{I_AI_B,J_AJ_B} = \delta_{I_BJ_B} M_{I_AJ_A}^A + \delta_{I_AJ_A} M_{I_BJ_B}^B \tag{59}$$

It should be emphasized once again that these results do not presuppose exact CC ground states, but apply as well to the (systematic) CC approximations.

The separability structure of $\boldsymbol{M}$ reflects once more the different quality of the left and right bCC expansion manifolds. While the LL triangular is separable, the UR triangular displays the non-separable CI-type structure of Fig. 2. What are the consequences for excitation energies and eigenvectors? Notwithstanding the apparently non-separable block structure of $\boldsymbol{M}$, the bCC excitation energies are obtained in a separable way [8]. It is readily seen that the characteristic polynomial for the fragment secular matrix $\boldsymbol{M}^A$ is a factor in the full characteristic polynomial associated with $\boldsymbol{M}$. Accordingly, the eigenvalues (excitation energies) of fragment A are a subset of the eigenvalues of the full secular matrix $\boldsymbol{M}$. This means that the energies of local excitations are separable quantities: the bCC results do not depend on whether the method is applied to the fragment or the composite system.

For the eigenvectors, one will expect different separability properties in the left and right manifolds. In fact, the right eigenvectors are separable, as shown in Fig. 4. For a local excitation n, say on fragment A, the only non-vanishing components are fragment-A components $\underline{X}_{An}$, and since $\boldsymbol{M}^A\underline{X}_{An} = \omega_n\underline{X}_{An}$ it is readily established that the fragment-A part of $\underline{X}_n$ is equal to the corresponding fragment-A eigenvector, $\underline{X}_{An} = \underline{X}_n^A$. More explicitly, the separability properties of right eigenvectors may be written as

$$X_{I_An} = X_{I_An}^A, \quad X_{I_Bn} = X_{I_ABn} = 0 \tag{60}$$

assuming here a fragment-A excitation, $n = n_A$.

For the left eigenvectors $\underline{Y}_n$ the fragment-A eigenvector is recovered by the A part of the full eigenvector, $\underline{Y}_{An} = \underline{Y}_n^A$. The local fragment-$B$ components vanish, $Y_{I_Bn} = 0$, but there are non-vanishing non-local components, $Y_{I_AB,n} \neq 0$. These non-local components are related to the local ones according to

$$\underline{Y}_{AB,n}^\dagger = \underline{Y}_{An}^\dagger \boldsymbol{M}_{A,AB}(\omega_n - \boldsymbol{M}_{AB,AB})^{-1} \tag{61}$$

This means that for a local excitation, say on A ($n = n_A$), the left eigenstate will take on the form

$$\left\langle\Psi_n^{(l)}\right| = \sum_{I_A} Y_{I_An}^* \langle\overline{\Phi}_{I_A}^A|\langle\Phi_0^B| + \sum_{I_AI_B} Y_{I_AI_B,n}^* \langle\overline{\Phi}_{I_A}^A|\langle\overline{\Phi}_{I_B}^B| \tag{62}$$

where $Y_{I_An} = Y_{I_An}^A$. In the exact (full) bCC result, this transforms into the product of the excited fragment-A state and dual ground state of fragment B (see Sect. 4.5).

4.2 Transition moments: truncation errors

Now, we are in the position to examine the truncation errors in the transition moments. Let us first consider the *left transition moments* (Eq. 45),

$$T_n^{(l)} = \langle\Psi_n^{(l)}|\hat{D}|\Psi_0^{cc}\rangle \tag{63}$$

which may be written more explicitly as scalar products

$$T_n^{(l)} = \underline{Y}_n^\dagger \underline{F}^{(l)} \tag{64}$$

of the left eigenvector $\underline{Y}_n$ and a vector $\underline{F}^{(l)}$ of basis set transition moments,

$$F_I^{(l)} = \langle\overline{\Phi}_I|\hat{D}|\Psi_0^{cc}\rangle \tag{65}$$

associated with the biorthogonal (left) basis states. The basis set transition moments, being part of the general bCC representation of the one-particle operator $\hat{D}$, exhibit canonical order relations

$$O\left[\underline{F}_\mu^{(l)}\right] = \mu - 1 \tag{66}$$

as shown in Fig. 5b. A proof of these order relations is given in Appendix 1. The scalar product (64) combines the left eigenvector components with the left basis set transition moments. This means that the (lowest) PT order associated with a specific class μ of eigenvector components is given by $O[\underline{Y}_\mu^\dagger \underline{F}_\mu^{(l)}] = O[\underline{Y}_\mu] + O[\underline{F}_\mu^{(l)}]$. Accordingly, the truncation after class μ leads to an error of the order $O[\underline{Y}_{\mu+1}] + O[\underline{F}_{\mu+1}^{(l)}]$. In the case of singly

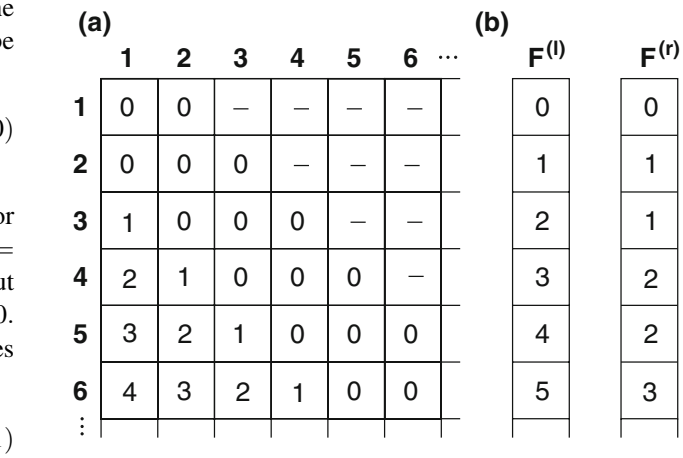

Fig. 5 **a** Order relations of the bCC representation $\boldsymbol{D}$ of a one-particle operator $\hat{D}$. Block structure and entries as in Figs. 1 and 3. **b** Order relations of the left and right basis set transition moments (see text)

excited states, the CI-type order relations of the left eigenvectors (Fig. 3b) lead to the TEO formula (53). However, so far we have disregarded the effect of truncations in the CC ground state. For example, there are first-order contributions in $\underline{F}_1^{(l)}$ (that is the p–h-components of $\underline{F}^{(l)}$) associated with the $2p$–$2h$ cluster operator $\hat{T}_2$ in the CC expansion of $|\Psi_0^{\rm cc}\rangle$. In conjunction with $\underline{Y}_1$, being of zeroth order, this gives rise to a first-order truncation error in the left transition moments if the ground-state CC expansion does not comprise the $2p$–$2h$ cluster operator. This can readily be generalized, noting that the $\hat{T}_\mu$ cluster operators are of the PT order $\mu - 1$. This means that in the class μ components of the F vector, $\underline{F}_\mu^{(l)}$, there are μth order contributions arising from the T operators of class $\mu + 1$. Depending on the respective lowest order in the eigenvector components of class μ, $\underline{Y}_\mu$, this leads to an additional truncation error, the order of which is by 1 smaller than that arising from the eigenvector truncation. The overall truncation errors for singly excited states are given by the following formula:

$$O_{\rm TE}(\mu) = \begin{cases} \frac{3}{2}\mu, & \mu \text{ even} \\ \frac{3}{2}\mu - \frac{1}{2}, & \mu \text{ odd} \end{cases} \tag{67}$$

In a similar way, one may analyze the bCC truncation errors for doubly and higher excited states; general TEO formulas are given in Appendix (bCC eigenvector matrices).

Likewise, the *right transition moments* (Eq. 46)

$$\begin{aligned} T_n^{(r)} &= \langle \overline{\Psi}_0 | \hat{D} | \Psi_n^{(r)} \rangle \\ &= x_n \langle \overline{\Psi}_0 | \hat{D} | \Psi_0^{\rm cc} \rangle + \sum_I F_I^{(r)} X_{In} \end{aligned} \tag{68}$$

can be written as scalar products of the extended right eigenvectors $\underline{X}'_n$ (see Eq. 38) and a vector $\underline{F}^{(r)}$ of the right basis set transition moments,

$$F_I^{(r)} = \langle \overline{\Psi}_0 | \hat{D} | \Psi_I^0 \rangle, \tag{69}$$

associated here with the CC states of right expansion manifold. In Eq. 68, the ground-state contribution ($I = 0$) is written separately.

Let us consider the second term on the RHS of Eq. 68, which will be seen to determine the overall truncation errors. Using the expansion (35) of the dual ground state, this term can be written as

$$\sum_I F_I^{(r)} X_{In} = \sum_I \langle \Phi_0 | \hat{D} | \Psi_I^0 \rangle X_{In} + \underline{Y}_0^\dagger \boldsymbol{D} \underline{X}_n \tag{70}$$

where $\boldsymbol{D}$ is the bCC representation of $\hat{D}$,

$$D_{IJ} = \langle \overline{\Phi}_I | \hat{D} | \Psi_J^0 \rangle \tag{71}$$

The order relations of $\boldsymbol{D}$ are shown in Fig. 5 (see Appendix 1 for a proof). The summation in the first term on the RHS of Eq. 70 is restricted to p–h components, $[I] = 1$, because $\langle \Phi_0 | \hat{D} | \Psi_I^0 \rangle = 0$ for $[I] > 1$, and, thus, does not cause a truncation error whatsoever. The second term can be written in the more explicit form

$$\underline{Y}_0^\dagger \boldsymbol{D} \underline{X}_n = \sum_{\kappa,\lambda} \underline{Y}_{\kappa 0}^* \boldsymbol{D}_{\kappa,\lambda} \underline{X}_{\lambda n}$$

reflecting the underlying partitioning with respect to excitation classes. To determine the truncation errors (at the level μ) one has to analyze the PT orders of the contributions with $\kappa = \mu + 1$, $\lambda \le \mu + 1$ and $\lambda = \mu + 1$, $\kappa \le \mu + 1$. This is described in Appendix 2, where general TEO formulas are derived. For singly excited states, $[n] = 1$, the TEOs of $\underline{Y}_0^\dagger \boldsymbol{D} \underline{X}_n$ are given by Eq. 67.

The first term on the RHS of Eq. 68, being the product of the ground-state admixture coefficient $x_n = -\underline{Y}_0^\dagger \underline{X}_n$, and the ground-state expectation value $\langle \overline{\Psi}_0 | \hat{D} | \Psi_0^{\rm cc} \rangle$, remains to be inspected. The truncation errors in the x_n coefficient have been specified in Eq. 190 of Appendix 2 (bCC eigenvector matrices), which become

$$O_{\rm TE}(\mu) = \begin{cases} \frac{3}{2}\mu + 1, & \mu \text{ even} \\ \frac{3}{2}\mu + \frac{1}{2}, & \mu \text{ odd} \end{cases} \tag{72}$$

in the case of singly excited states, $[n] = 1$. To determine the truncation errors in the factor $\langle \overline{\Psi}_0 | \hat{D} | \Psi_0^{\rm cc} \rangle$, we expand the dual ground state according to Eq. 35, which yields

$$\langle \overline{\Psi}_0 | \hat{D} | \Psi_0^{\rm cc} \rangle = \langle \Phi_0 | \hat{D} | \Psi_0^{\rm cc} \rangle + \underline{Y}_0^\dagger \underline{F}^{(l)} \tag{73}$$

Here, the first term is of zeroth order and does not induce a truncation error. The second term can be analyzed in a similar way as the left TMs above. Here the TEOs are given by

$$O_{\rm TE}(\mu) = \begin{cases} \frac{3}{2}\mu, & \mu \text{ even} \\ \frac{3}{2}\mu + \frac{1}{2}, & \mu \text{ odd} \end{cases} \tag{74}$$

Since for singly excited states ($[n] = 1$) x_n is (at least) of the second order, the overall truncation errors in the first term on the RHS of Eq. 68 are given by that of x_n (Eq. 72), exceeding those of the second term (Eq. 67) by one. We note that for singly excited states, the TEOs in the left and right transition moments are the same (see Table 1).

4.3 Transition moments: separability

The separability of the left transition moments (Eqs. 63–65) is easily established. According to

$$\begin{aligned} F_{I_A}^{(l)} &= \langle \overline{\Phi}_{I_A}^A | \langle \overline{\Phi}_0^B | \hat{D}_A + \hat{D}_B | \Psi_0^A \rangle | \Psi_0^B \rangle = \langle \overline{\Phi}_{I_A}^A | \hat{D}_A | \Psi_0^A \rangle \\ &= F_{I_A}^{(l)A} \end{aligned} \tag{75}$$

it is seen that for local excitations I_A, the basis set transition moments for fragment A are identical to the corresponding moments of the composite system. Moreover, the basis set transition moments for mixed excitations vanish,

$$F^{(l)}_{I_A I_B} = 0 \tag{76}$$

which means that the non-separable part of the left eigenvector does not come into play at all. Accordingly, for a local (fragment-A) excitation, $n = n_A$, we may write

$$T^{(l)}_n = \sum_{I_A} Y^*_{I_A n} F^{(l)A}_{I_A} = T^{(l)A}_n \tag{77}$$

where $T^{(l)A}_n$ is the left transition moment for fragment A. In deriving this result, we have assumed that the local components for the composite system eigenvectors are identical to the components of the corresponding fragment eigenvectors, $Y_{I_A n} = Y^A_{I_A n}$.

Whereas the left transition moments are separable notwithstanding the non-separable left eigenvectors, the right transition moments (Eqs. 68, 69), involving separable eigenvectors, prove not to be separable. The problem here arises from the use of the dual ground state $\langle\overline{\Psi}_0|$, more precisely from the fact that a factorization of the dual ground state,

$$\langle\overline{\Psi}_0| = \langle\overline{\Psi}^A_0|\langle\overline{\Psi}^B_0| \tag{78}$$

is attained only in the exact (full bCC) treatment. To better understand the problem, let us first assume factorization of $\langle\overline{\Psi}_0|$ and inspect $T^{(r)}_n$ for a local excitation, $n = n_A$:

$$T^{(r)}_n = x_n\langle\overline{\Psi}_0|\hat{D}|\Psi^{\mathrm{cc}}_0\rangle + \sum_{I_A} F^{(r)}_{I_A} X^A_{I_A n} \tag{79}$$

Here, the separability properties (60) of the right eigenvector $\underline{X}_n$ have been used; $F^{(r)}_I$ denote (right) basis set transition moments (Eq. 69). The ground-state component x_n of the right eigenvector in the first term on the RHS is always separable, since

$$x_n = -\underline{Y}^\dagger_0\underline{X}_n = -\underline{Y}^{A\dagger}_0\underline{X}^A_n = x^A_n \tag{80}$$

By contrast, the ground-state expectation value

$$\langle\overline{\Psi}_0|\hat{D}|\Psi^{\mathrm{cc}}_0\rangle = \langle\overline{\Psi}^A_0|\hat{D}_A|\Psi^A_0\rangle + \langle\overline{\Psi}^B_0|\hat{D}_B|\Psi^B_0\rangle \tag{81}$$

is a non-local quantity, involving both fragment A and B. It should be noted that the separation of the bCC ground-state expectation value into the sum of fragment expectation values not only holds for the exact (factorizing) dual ground state, but also for truncated expansions according to Eq. 84 (in this sense the bCC ground-state expectation values themselves are separable quantities). Being a product of a local and a non-local factor, however, the first term on the RHS of Eq. 79 is not separable. This means that the non-separable contribution $x_n\langle\overline{\Psi}^B_0|\hat{D}_B|\Psi^B_0\rangle$ in the first term of Eq. 79 must be cancelled by a corresponding contribution in the second term, to be identified in the following. For a local configuration, $I = I_A$, the right basis set transition moment (Eq. 69) becomes

$$F^{(r)}_{I_A} = \langle\overline{\Psi}^A_0|\hat{D}_A|\Psi^A_{I_A}\rangle + \langle\overline{\Psi}^A_0|\Psi^A_{I_A}\rangle\langle\overline{\Psi}^B_0|\hat{D}_B|\Psi^B_0\rangle \tag{82}$$

Obviously, $F^{(r)}_{I_A}$ is not separable. While the first term on the RHS is the fragment-A transition moment, $F^{(r)A}_{I_A} = \langle\overline{\Psi}^A_0|\hat{D}_A|\Psi^A_{I_A}\rangle$, the second term is a non-separable contribution involving fragment B. In the full bCC treatment, the two non-separable contributions in $T^{(r)}_n$ cancel each other. This is readily seen by inserting Eq. 82 in Eq. 79 and using that $\langle\overline{\Psi}^A_0|\Psi^A_{I_A}\rangle = Y^*_{I_A 0}$ and

$$\sum_{I_A} Y^*_{I_A 0} X^A_{I_A n} = -x^A_n \tag{83}$$

For truncated bCC expansions, on the other hand, the non-separable contributions will not compensate each other, giving rise to size-consistency errors in the computational results.

The non-separability of the right transition moments can be further elaborated by inspecting the general form of the dual ground state,

$$\langle\overline{\Psi}_0| = \langle\Phi^A_0|\langle\Phi^B_0| + \sum_{J_A} Y^*_{J_A 0}\langle\overline{\Phi}^A_{J_A}|\langle\Phi^B_0| + \sum_{J_B} Y^*_{J_B 0}\langle\Phi^A_0|\langle\overline{\Phi}^B_{J_B}| + \sum_{J_A J_B} Y^*_{J_A J_B,0}\langle\overline{\Phi}^A_{J_A}|\langle\overline{\Phi}^B_{J_B}| \tag{84}$$

applying both to truncated and full expansions. Here the local expansion coefficients are separable, that is, $Y_{J_A 0} = Y^A_{J_A 0}$ and $Y_{J_B 0} = Y^B_{J_B 0}$. This follows from Eq. 34 and the separability properties of $\boldsymbol{M}$ and $\underline{v}$ (see below). Using the expansion (84), the right basis set transition moments take on the form

$$F^{(r)}_{I_A} = F^{(r)A}_{I_A} + Y^*_{I_A 0}\langle\Phi^B_0|\hat{D}_B|\Psi^B_0\rangle + \sum_{J_B} Y^*_{I_A J_B,0}\langle\overline{\Phi}^B_{J_B}|\hat{D}_B|\Psi^B_0\rangle \tag{85}$$

With the help of Eqs. 80 and 81, we finally arrive at the expression

$$T^{(r)}_n = T^{(r)A}_n + x^A_n\left(\langle\overline{\Psi}^B_0|\hat{D}_B|\Psi^B_0\rangle - \langle\Phi^B_0|\hat{D}_B|\Psi^B_0\rangle\right) + \sum_{I_A J_B} X_{I_A n} Y^*_{I_A J_B,0}\langle\overline{\Phi}^B_{J_B}|\hat{D}_B|\Psi^B_0\rangle \tag{86}$$

for the right transition moments. Here $T^{(r)A}_n$ denotes the right transition moment for fragment A. The non-separable contributions are identified as the second and third term on the RHS of Eq. 86. These terms cancel each other if the non-local eigenvector components factorize, that is,

$$Y_{I_A J_B,0} = Y_{I_A 0} Y_{J_B 0} \tag{87}$$

This can be seen by recalling that $\sum Y^*_{I_A 0} X_{I_A n} = -x^A_n$ and $\langle\overline{\Psi}^B_0| = \langle\Phi^B_0| + \sum Y^*_{J_B 0}\langle\overline{\Phi}^B_{J_B}|$. It should be clear, however, that the factorization (87) of the non-local eigenvector components is equivalent to the factorization (78) of the

dual ground state (84), applying only to the full bCC expansion.

It may be of interest to see how the factorization of the exact dual ground-state eigenvector components derives from the explicit expression (Eq. 34),

$$\underline{Y}_0^{\dagger} = -\underline{v}^{\mathrm{t}}\mathbf{M}^{-1}$$

As is readily established, the local contributions to $\underline{v}$ are separable,

$$v_{I_A} = \langle \Phi_0^A | \hat{H}_A | \Psi_{I_A}^A \rangle = v_{I_A}^A \tag{88}$$

and the mixed components vanish,

$$v_{I_A I_B} = 0 \tag{89}$$

The inverse of the bCC secular matrix is given by

$$\mathbf{M}^{-1} = \begin{pmatrix} \boldsymbol{M}_{AA}^{-1} & - & \boldsymbol{P}_{A,AB} \\ - & \boldsymbol{M}_{BB}^{-1} & \boldsymbol{Q}_{A,AB} \\ - & - & \boldsymbol{M}_{AB,AB}^{-1} \end{pmatrix} \tag{90}$$

where

$$\boldsymbol{P}_{A,AB} = -\boldsymbol{M}_{AA}^{-1}\boldsymbol{M}_{A,AB}\boldsymbol{M}_{AB,AB}^{-1} \tag{91}$$

$$\boldsymbol{Q}_{A,AB} = -\boldsymbol{M}_{BB}^{-1}\boldsymbol{M}_{B,AB}\boldsymbol{M}_{AB,AB}^{-1} \tag{92}$$

so that, according to Eq. 34, the non-local eigenvector components can be written as

$$\underline{Y}_{AB,0} = (\underline{v}_A^{\mathrm{t}}\boldsymbol{M}_{AA}^{-1}\boldsymbol{M}_{A,AB} + \underline{v}_B^{\mathrm{t}}\boldsymbol{M}_{BB}^{-1}\boldsymbol{M}_{B,AB})\boldsymbol{M}_{AB,AB}^{-1} \tag{93}$$

To proceed, the secular matrix blocks, $\boldsymbol{M}_{AB,AB}$, $\boldsymbol{M}_{A,AB}$, and $\boldsymbol{M}_{B,AB}$, have to be further evaluated. Using a somewhat symbolic, but largely self-explanatory, notation, these blocks may be written as

$$\boldsymbol{M}_{AB,AB} = \mathbf{1}_B \times \boldsymbol{M}_{AA} + \mathbf{1}_A \times \boldsymbol{M}_{BB} \tag{94}$$

$$\boldsymbol{M}_{A,AB} = \mathbf{1}_A \times \underline{v}_B^{\mathrm{t}}, \quad \boldsymbol{M}_{B,AB} = \mathbf{1}_B \times \underline{v}_A^{\mathrm{t}} \tag{95}$$

Proceeding at this symbolic level, the desired result is readily obtained as follows:

$$\begin{aligned} \underline{Y}_{AB,0} &= \underline{v}_A^{\mathrm{t}} \times \underline{v}_B^{\mathrm{t}}(\boldsymbol{M}_{AA}^{-1} + \boldsymbol{M}_{BB}^{-1})\boldsymbol{M}_{AB,AB}^{-1} \\ &= \underline{v}_A^{\mathrm{t}} \times \underline{v}_B^{\mathrm{t}}\boldsymbol{M}_{AA}^{-1}\boldsymbol{M}_{BB}^{-1}(\mathbf{1}_B \times \boldsymbol{M}_{AA} + \mathbf{1}_A \times \boldsymbol{M}_{BB})\boldsymbol{M}_{AB,AB}^{-1} \\ &= \underline{v}_A^{\mathrm{t}}\boldsymbol{M}_{AA}^{-1} \times \underline{v}_B^{\mathrm{t}}\boldsymbol{M}_{BB}^{-1} \\ &= \underline{Y}_{A0} \times \underline{Y}_{B0} \end{aligned} \tag{96}$$

In a more stringent manner, the preceding computation can be performed on the matrix-element level, that is, by explicitly expanding all matrix multiplications. Here, the symbolic treatment according to Eqs. 93–96 may serve as a guidance.

Let us recall once again that a factorization of the dual ground state cannot be expected if the configuration space is truncated. For example, assume a configuration space extending through double excitations and let I_A and J_B denote double excitations on fragment A and B, respectively. Then the factorization according to Eq. 87 would require that the configuration space of the system as a whole comprises quadruple excitations of the type $I_A J_B$, which, however, are not available in the truncated configuration manifold.

4.4 CCLR form of right transition moments

The derivation of the excited-state CC equations in the framework of the linear response theory leads to the following separable, if more involved, expression for the right transition moment [7]:

$$\begin{aligned} T_n^{(r)} = \langle \overline{\Psi}_0 | [\hat{D}, \hat{C}_n] | \Psi_0^{\mathrm{cc}} \rangle - \sum_{I,J} \langle \overline{\Psi}_0 | [[\hat{H}, \hat{C}_I], \hat{C}_n] | \Psi_0^{\mathrm{cc}} \rangle \\ \times (\boldsymbol{M} + \omega_n)_{IJ}^{-1} \langle \overline{\Phi}_J | \hat{D} | \Psi_0^{\mathrm{cc}} \rangle \end{aligned} \tag{97}$$

Here,

$$\hat{C}_n = \sum X_{Kn}\hat{C}_K \tag{98}$$

denotes an excitation operator associated with the the nth (right) excited state: $|\Psi_n^{(r)}\rangle = x_n|\Psi_0^{\mathrm{cc}}\rangle + \hat{C}_n|\Psi_0^{\mathrm{cc}}\rangle$. Since the CCLR derivation starts out from a separable expression for a time-dependent ground-state expectation value, one may expect that the separability properties will be maintained in the further development. Nevertheless, it is reassuring to see directly that the CCLR form of the right transition moments is separable [19]. Moreover, one will expect that the ordinary bCC (68) and the CCLR (97) expressions, while being of quite different form, must somehow become equivalent in the exact (full) bCC treatment. The absolutely non-trivial proof of this equivalence has been accomplished by Koch et al. [19]. In the following, we will briefly review the separability of the CCLR right transition moments. The equivalence of the two transition moment expressions is addressed in Appendix 3.

To show the separability of the right CCLR transition moments, we will suppose the general expansion (84) of the dual ground state, which holds both for approximate and exact (full) bCC treatments. Let n be a local excitation on fragment A ($n = n_A$). According to the separability of the right eigenvector, $\hat{C}_n$ consists only of local excitation operators, $\hat{C}_n = \sum X_{I_A}\hat{C}_{I_A}$. Now it is easy to see that the first (commutator) term on the RHS of Eq. 97 is separable. Since $[\hat{D}, \hat{C}_{I_A}] = [\hat{D}_A, \hat{C}_{I_A}]$, the commutator becomes a local (fragment-A) operator, say $\hat{O}_A$. As a consequence, in the matrix element $\langle \overline{\Psi}_0 | \hat{O}_A | \Psi_0^{\mathrm{cc}} \rangle$, the fragment B and non-local (AB) contributions in the expansion of $\langle \overline{\Psi}_0 |$ are projected out, that is, $\langle \overline{\Psi}_0 | \hat{O}_A | \Psi_0^{\mathrm{cc}} \rangle = \langle \overline{\Psi}_0^A | \hat{O}_A | \Psi_0^A \rangle$. Now, let us consider the second term on the RHS of Eq. 97, involving a double summation running over generic configuration indices I,J. The double commutator, involving the

fragment-A excitation operator $\hat{C}_n$ and excitation operators $\hat{C}_I$, leads to a restriction on the indices I: there are no (non-vanishing) contributions for $I = I_B$ (fragment-B excitations), since $[\hat{H}, \hat{C}_{I_B}] = [\hat{H}_B, \hat{C}_{I_B}]$ and $[[\hat{H}_B, \hat{C}_{I_B}], \hat{C}_{n_A}] = 0$. But what about contributions associated with non-local configurations $I = I_{AB}$, not excluded by the double commutator term? To proceed, let us inspect the matrix elements of $(\boldsymbol{M} + \omega_n)^{-1}$. According to the separability structure of this matrix (see Eq. 90), the only non-vanishing matrix elements of the type (I_{AB}, J) are those where the J index is non-local too, $J = J_{AB}$. However, the non-local left basis set transition moments, $F_J^{(l)} = \langle\overline{\Phi}_J|\hat{D}|\Psi_0^{\rm cc}\rangle$, appearing as factors on the RHS of Eq. 97, vanish for non-local (mixed) configurations J_{AB} (see Eq. 76), which means that non-local configurations can be excluded in both the J and the I summations. To conclude, for a local excitation $n = n_A$, the double summation on the RHS of Eq. 97 runs only over local fragment A configurations I_A, J_A. With this restriction, it is readily established that the three ingredients on the RHS of Eq. 97, i.e., the double commutator matrix elements, the matrix inverse and the left basis set transition moments, are separable. They give the same results irrespective of being computed for the entire system or for fragment A only.

4.5 Excited-state properties and transition moments

So far, we have discussed ground-to-excited state transition moments required to compute spectral intensities. Now, we will turn to excited-state expectation values (properties) for physical quantities of interest, e.g., excited-state dipole moments, and, more generally, transition moments associated with transitions between two excited states.

In the bCC form, the general expression

$$T_{nm} = \langle\Psi_n|\hat{D}|\Psi_m\rangle \tag{99}$$

for excited-state transition moments becomes

$$\begin{aligned} T_{nm} &= \langle\Psi_n^{(l)}|\hat{D}|\Psi_m^{(r)}\rangle \\ &= x_m\langle\Psi_n^{(l)}|\hat{D}|\Psi_0^{\rm cc}\rangle + \underline{Y}_n^{\dagger}\boldsymbol{D}\underline{X}_m \end{aligned} \tag{100}$$

Here, $\boldsymbol{D}$ denotes the bCC representation (71) of a given operator $\hat{D}$. The order structure of $\boldsymbol{D}$ is shown in Fig. 5, supposing here that $\boldsymbol{D}$ is a one-particle operator; for a proof of these order relations see Appendix 1.

The truncation errors of the T_{nm} matrix elements are governed by the second term on the RHS of Eq. 100. The secondary role of the first term can be seen in a similar way as in the right transition moments discussed in Sect. 4.2. We here skip the corresponding analysis of the first term, noting only that the order relations of two constituents, that is, the ground-state admixture coefficient x_m and the left (ground-to-excited state) transition moment $T_n^{(l)}$, have already been established in Sect. 4.2. The truncation errors associated with the second term, being of the form of a vector × matrix × vector product, can be derived from the order relations of $\boldsymbol{D}$ and the respective left and right eigenvectors, as described in more detail in Appendix 2 (bCC eigenvector matrices). In the case of singly excited states ($[n] = [m] = 1$), the general formula (189) in Appendix 2 simplifies to

$$O_{\rm TE}(\mu) = \begin{cases} \frac{3}{2}\mu - 1, & \mu \text{ even} \\ \frac{3}{2}\mu - \frac{1}{2}, & \mu \text{ odd} \end{cases} \tag{101}$$

As the comparison with Eq. 53 shows, the excited-state transition moments for singly excited states (and a one-particle transition operator) have larger truncation errors (i.e., lower TEOs) than the excitation energies and ground-to-excited state transition moments.

To discuss the separability, we consider once more local excitations on fragment A, that is, $n = n_A$, $m = m_A$. In the exact case, where the left and right excited states can be written as fragment state products,

$$\begin{aligned} \langle\Psi_n^{(l)}| &= \langle\Psi_n^{(l)A}|\langle\overline{\Psi}_0^B| \\ |\Psi_m^{(r)}\rangle &= |\Psi_m^{(r)A}\rangle|\Psi_0^B\rangle \end{aligned}$$

the excited-state transition moments take on the manifestly separable form,

$$T_{nm} = T_{nm}^A + \delta_{nm}\langle\overline{\Psi}_0^B|\hat{D}_B|\Psi_0^B\rangle \tag{102}$$

where

$$T_{nm}^A = \langle\Psi_n^{(l)A}|\hat{D}_A|\Psi_m^{(r)A}\rangle \tag{103}$$

is the transition moment for fragment A. Note that for diagonal (property) matrix elements ($n = m$), there is a contribution $\langle\overline{\Psi}_0^B|\hat{D}_B|\Psi_0^B\rangle$, corresponding to the ground-state expectation value of $\hat{D}$ for fragment B.

Now let us analyze Eq. 100 in the case of a truncated bCC representation. The first term on the RHS of Eq. 100 is separable,

$$x_m T_n^{(l)} = x_m^A T_n^{(l)A} \tag{104}$$

as has already been shown in the preceding section. In the second term,

$$T'_{nm} = \underline{Y}_n^{\dagger}\boldsymbol{D}\underline{X}_m \tag{105}$$

the separability structure of $\boldsymbol{D}$ comes into play. As in the case of the bCC secular matrix (see Sect. 4.1), the separability structure of $\boldsymbol{D}$ can easily be derived. The result is shown in Fig. 6. The relevant sub-blocks $\boldsymbol{D}_{AA}$ and $\boldsymbol{D}_{AB,A}$ are given by

$$\boldsymbol{D}_{AA} = \boldsymbol{D}_{AA}^A + \mathbf{1}_A\langle\Phi_0^B|\hat{D}_B|\Psi_0^B\rangle \tag{106}$$

$$\boldsymbol{D}_{AB,A} = \mathbf{1}_A \times \underline{F}_B^{(l)} \tag{107}$$

	A	B	AB
A	$\boldsymbol{D}_{AA}$	–	$\boldsymbol{D}_{A,AB}$
B	–	$\boldsymbol{D}_{BB}$	$\boldsymbol{D}_{B,AB}$
AB	$\boldsymbol{D}_{AB,A}$	$\boldsymbol{D}_{AB,B}$	$\boldsymbol{D}_{AB,AB}$

Fig. 6 **a** Block structure of the bCC representation $\boldsymbol{D}$ of a general operator $\hat{D}$ with respect to the separate fragment model (as in Figs. 2 and 4)

Here $\underline{F}_B^{(l)} = \underline{F}_B^{(l)B}$ is the vector of left basis set transition moments for fragment B, as in Eq. 75. Using these expressions, Eq. 105 becomes

$$T'_{nm} = \underline{Y}^{\dagger}_{An}\boldsymbol{D}_{AA}\underline{X}_{Am} + \underline{Y}^{\dagger}_{AB,n}\boldsymbol{D}_{AB,A}\underline{X}_{Am} \tag{108}$$

where

$$\underline{Y}^{\dagger}_{AB,n} = \underline{Y}^{\dagger}_{An}\boldsymbol{M}_{A,AB}(\omega_n - \boldsymbol{M}_{AB,AB})^{-1} \tag{109}$$

is the non-local part of the left eigenvector $\underline{Y}^{\dagger}_n$, as specified by Eq. 61. Let us now first consider the non-diagonal case, $n \neq m$, where the left and right eigenvectors are orthogonal. Using the result

$$\underline{Y}^{\dagger}_{An}\boldsymbol{D}_{AA}\underline{X}_{Am} = \underline{Y}^{A\dagger}_{n}\boldsymbol{D}^{A}\underline{X}^{A}_{m} \tag{110}$$

for the first term on the RHS of Eq. 108, as well as Eq. 104, leads to the following expression:

$$T_{nm} = T^{A}_{nm} + \underline{Y}^{\dagger}_{AB,n}\boldsymbol{D}_{AB,A}\underline{X}_{Am} \tag{111}$$

This means that T_{nm} is not separable due to the second term on the RHS arising from the non-local left eigenvector contributions. In the exact (full bCC) treatment, these non-local eigenvector components factorize according to

$$Y_{I_AI_B,n} = Y_{I_An}Y_{I_B0} \tag{112}$$

that is, they form products of excited state and ground-state eigenvector components for fragment A and B, respectively. Then the non-separable term vanishes due to the orthogonality of the fragment eigenvectors, $\underline{Y}^{A\dagger}_n\underline{X}^{A}_m = 0$ and the form of $\boldsymbol{D}_{AB,A}$ (Eq. 107).

For the diagonal case, $n = m$, the result is

$$T_{nn} = T^{A}_{nn} + \sum_{I_AI_B} Y^{*}_{I_AI_B}X_{I_A}\langle\overline{\Phi}^{B}_{I_B}|\hat{D}_B|\Psi^{B}_0\rangle \tag{113}$$

where again Eq. 107 has been used. Only on factorization of the non-local eigenvector components (Eq. 112), the correct result of Eq. 102 is obtained.

Again we may perform a brief symbolic calculation to demonstrate the factorization (112) of the exact excited-state eigenvector components The starting point is Eq. 61, where we may replace $\boldsymbol{M}_{A,AB}$ according to

$$\boldsymbol{M}_{A,AB} = \boldsymbol{1}_A \times \underline{v}^{t}_B = -\boldsymbol{1}_A \times \underline{Y}^{\dagger}_{B0}\boldsymbol{M}_{BB} \tag{114}$$

to give

$$\underline{Y}^{\dagger}_{AB,n} = -\underline{Y}^{\dagger}_{An} \times \underline{Y}^{\dagger}_{B0}\boldsymbol{M}_{BB}(\omega_n - \boldsymbol{M}_{AB,AB})^{-1} \tag{115}$$

Here, the general relation (35), specialized to fragment B,

$$\underline{Y}^{\dagger}_{B0} = -\underline{v}^{t}_B\boldsymbol{M}^{-1}_{BB} \tag{116}$$

has been used in Eq. 114. Since $\underline{Y}_{An}$ is an eigenvector of $\boldsymbol{M}_{AA}$, it follows that

$$\underline{Y}^{\dagger}_{An}(\omega_n - \boldsymbol{M}_{AB,AB}) = \underline{Y}^{\dagger}_{An}(\boldsymbol{M}_{AA} - \boldsymbol{M}_{AB,AB}) \tag{117}$$

$$= -\underline{Y}^{\dagger}_{An} \times \boldsymbol{M}_{BB} \tag{118}$$

and, as a consequence

$$\underline{Y}^{\dagger}_{An}(\omega_n - \boldsymbol{M}_{AB,AB})^{-1} = -\underline{Y}^{\dagger}_{An} \times \boldsymbol{M}^{-1}_{BB} \tag{119}$$

Using the latter result in Eq. 115 gives

$$\underline{Y}^{\dagger}_{AB,n} = \underline{Y}^{\dagger}_{An} \times \underline{Y}^{\dagger}_{B0} \tag{120}$$

The factorization of the non-local eigenvector components is of course equivalent to the factorization $\langle\Psi^{(l)}_n| = \langle\Psi^{(l)A}_n|\langle\overline{\Psi}^{B}_0|$ of the expansion (62).

As we have seen, the ordinary bCC expression (100) for the excited-state transition moments and properties is non-separable, which here is due to the non-separable components in the left excited-state eigenvectors. Again, the CCLR approach results in an alternative separable expression [7], reading

$$T_{nm} = \langle\overline{\Psi}^{(l)}_n|[\hat{D},\hat{C}_m]|\Psi^{cc}_0\rangle - \sum_{I,J}\langle\overline{\Psi}^{(l)}_n|[[\hat{H},\hat{C}_I],\hat{C}_m]|\Psi^{cc}_0\rangle \times (\boldsymbol{M} + \omega_{mn})^{-1}_{IJ}\langle\overline{\Phi}_J|\hat{D}|\Psi^{cc}_0\rangle + \delta_{nm}\langle\overline{\Psi}_0|\hat{D}|\Psi^{cc}_0\rangle \tag{121}$$

where $\omega_{mn} = \omega_m - \omega_n$. The separability of this form can be shown in the same manner as in the case of the ground-to-excited-state transition moments (Sect. 4.4). The equivalence of the CCLR form (121) and the ordinary bCC expression of the excited-state transition moments is briefly addressed in Appendix 3.

5 Hermitian intermediate state representation

The bCC representation is a mixed or hybrid representation made up of the CC states and the associated biorthogonal

states. Whereas the (correlated excited) CC states are genuine intermediate states, being based on the correlated ground state, the biorthogonal states are essentially of the CI-type, that is, excited HF configurations. As was analyzed in the previous section, the use of the biorthogonal CI-type states as the left expansion manifold downgrades to a certain extent the truncation errors and separability properties of the bCC computational schemes. For the purpose of comparison, we will briefly inspect the properties of a hermitian intermediate state representation (ISR), specifically the ADC-ISR approach [18, 24–26, 32], in the following.

As the bCC representation, the ADC-ISR approach starts from the correlated excited states (Eq. 15)

$$|\Psi_J^0\rangle = \hat{C}_J|\Psi_0\rangle \tag{122}$$

where $|\Psi_0\rangle$ now refers to the normalized ground state rather than to the CC parametrization. The correlated excited states (CES) can then be transformed into orthonormal intermediate states (IS),

$$|\Psi_J^0\rangle \longrightarrow |\tilde{\Psi}_J\rangle$$

via a (formal) Gram–Schmidt orthogonalization procedure, in which successively higher CES classes μ are orthogonalized with respect to the already constructed lower IS classes $\nu = 1, 2, \ldots, \mu - 1$. Within a given excitation class, symmetric orthonormalization is adopted. All the states are explicitly orthogonalized to the exact ground state, forming a zeroth excitation class ($\mu = 0$). As a result of this (so far purely formal) procedure, one obtains an orthonormal set of intermediate states $|\tilde{\Psi}_J\rangle$,

$$\langle\tilde{\Psi}_I|\tilde{\Psi}_J\rangle = \delta_{IJ} \tag{123}$$

being, moreover, orthogonal to the exact ground-state, $\langle\tilde{\Psi}_J|\Psi_0\rangle = 0$.

Representing the (shifted) Hamiltonian $\hat{H} - E_0$ in terms of these intermediate states gives rise to a hermitian secular matrix $\mathbf{M}$,

$$M_{IJ} = \langle\tilde{\Psi}_I|\hat{H} - E_0|\tilde{\Psi}_J\rangle \tag{124}$$

and the associated hermitian eigenvalue problem,

$$\mathbf{MX} = \mathbf{X\Omega}, \quad \mathbf{X}^\dagger\mathbf{X} = \mathbf{1} \tag{125}$$

Here $\mathbf{\Omega}$ is the diagonal matrix of excitation energies, $\omega_n = E_n - E_0$, and $\mathbf{X}$ denotes the matrix of (column) eigenvectors. The nth excited state can be expanded as

$$|\Psi_n\rangle = \sum_J X_{Jn}|\tilde{\Psi}_J\rangle \tag{126}$$

in terms of the intermediate states and the eigenvector components X_{Jn}. The transition moments take on the form

$$T_n = \langle\Psi_n|\hat{D}|\Psi_0\rangle = \sum_J F_J X_{Jn}^* \tag{127}$$

where

$$F_J = \langle\tilde{\Psi}_J|\hat{D}|\Psi_0\rangle \tag{128}$$

are denoted as IS transition moments.

To obtain practical computational schemes, the Gram–Schmidt procedure is used together with Rayleigh–Schrödinger (RS) PT for $|\Psi_0\rangle$ and E_0, generating explicit perturbation expansions for the secular matrix

$$\boldsymbol{M} = \boldsymbol{M}^{(0)} + \boldsymbol{M}^{(1)} + \boldsymbol{M}^{(2)} + \cdots \tag{129}$$

and the IS transition moments

$$\underline{F} = \underline{F}^{(0)} + \underline{F}^{(1)} + \underline{F}^{(2)} + \cdots \tag{130}$$

By truncating the IS manifolds and the perturbation expansions for the secular matrix elements and IS transition moments in a systematic and consistent manner, one arrives at a hierarchy of ADC(n) approximations, where n indicates that both the energies and transition moments of the lowest excitation class (singly excited states) are treated consistently through order n. An alternative and, beyond second order, preferable derivation of the ADC-ISR perturbation expansions is the original ADC formulation [24, 25] based on diagrammatic PT for the polarization propagator [33].

As a distinctive feature of the ADC-ISR, the canonical order structure [18] applies to the entire secular matrix (see Fig. 7),

$$M_{IJ} \sim O(|[I] - [J]|) \tag{131}$$

and, as a consequence, also to the eigenvector matrix $\boldsymbol{X}$:

$$X_{IJ} \sim O(|[I] - [J]|) \tag{132}$$

In analogy to the last paragraph of Appendix 2 (CI eigenvector matrix), one readily obtains the truncation error formula

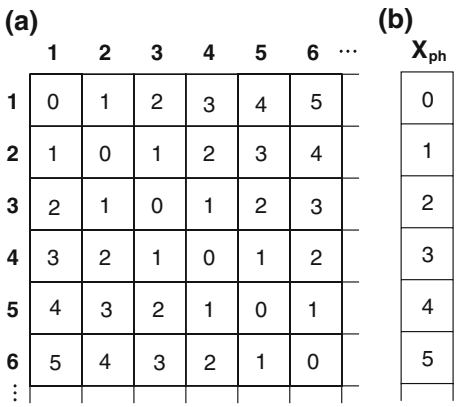

Fig. 7 **a** Order relations of the ADC-ISR secular matrix $\boldsymbol{M}$. Block structure and entries as in Figs. 1 and 3. **b** Order relations of ADC-ISR eigenvectors for singly excited states

$$O_{\mathrm{TE}}^{[n]}(\mu) = 2O[\underline{X}_{\mu+1,n}] = 2(\mu - [n] + 1), \quad \mu \geq [n] \tag{133}$$

for the excitation energies. Here, $[n]$ denotes the class of the excited state n (as established by the PT parentage), and μ specifies the truncation level of the ISR expansion manifold. In a similar way, the canonical order relations

$$F_J \sim O([J] - 1) \tag{134}$$

for the IS transition moments lead (via Eq. 127) to the following expression for the truncation error in the transition moments:

$$O_{\mathrm{TE}}^{[n]}(\mu) = O[\underline{F}_{\mu+1}] + O[\underline{X}_{\mu+1,n}] = 2\mu - [n] + 1, \quad \mu \geq [n] \tag{135}$$

For the lowest excitation class of the singly excited states ($[n] = 1$), the truncation error is 2μ, both for the excitation energies and the transition moments. In Table 1, the errors for the six lowest truncation levels are compared to the corresponding CI and bCC values.

The treatment of excited-state properties and transition moments,

$$T_{nm} = \langle \Psi_n | \hat{D} | \Psi_m \rangle = \underline{X}_n^{\dagger} \boldsymbol{D} \underline{X}_m \tag{136}$$

is based on the ISR of a general one-particle operator,

$$D_{IJ} = \langle \tilde{\Psi}_I | \hat{D} | \tilde{\Psi}_J \rangle \tag{137}$$

Like the secular matrix (Eq. 129), the IS property matrix $\boldsymbol{D}$ is subject to a perturbation expansion,

$$\boldsymbol{D} = \boldsymbol{D}^{(0)} + \boldsymbol{D}^{(1)} + \boldsymbol{D}^{(2)} + \cdots \tag{138}$$

Here the "shifted canonical" order relations

$$D_{IJ} \sim O(|[I] - [J]| - 1), \quad |[I] - [J]| \geq 1 \tag{139}$$

apply, reflecting that a one-particle operator can couple HF (zeroth order) excitations of successive excitation classes. The product $\underline{Z}_n = \boldsymbol{D}\underline{X}_n$ modifies the canonical order relations of an ADC-ISR eigenvector accordingly, that is,

$$Z_{In} \sim O([I] - [n] - 1), \quad [I] - [n] \geq 1 \tag{140}$$

This leads readily to the expression

$$O_{\mathrm{TE}}^{[n]}(\mu) = O[\underline{X}_{\mu+1,n}] + O[\underline{Z}_{\mu+1,n}] = 2(\mu - [n]) + 1, \quad \mu \geq [n] \tag{141}$$

for the truncation error of excited-state property matrix elements T_{nn}.

The ADC-ISR secular matrix is fully separable [18, 34]: it has a diagonal partitioning structure as shown in Fig. 8, and the diagonal blocks are identical with the corresponding fragment secular matrices, that is, $\boldsymbol{M}_{AA} = \boldsymbol{M}^{(A)}$. For a local excitation, say on fragment A, the fragment and entire system treatments give the same excitation energy, and the fragment eigenvector is part of the entire system eigenvector, in which all non-local components vanish ($X_{I_{B,n}} = X_{I_{AB,n}} = 0$). The IS transition moments are separable as well, $F_{I_A} = F_{I_A}^{(A)}$. Together with the separable eigenvectors this ensures size-consistent results for the ADC-ISR transition moments. The case of the excited-state properties and transition moments has been discussed in Ref. [32].

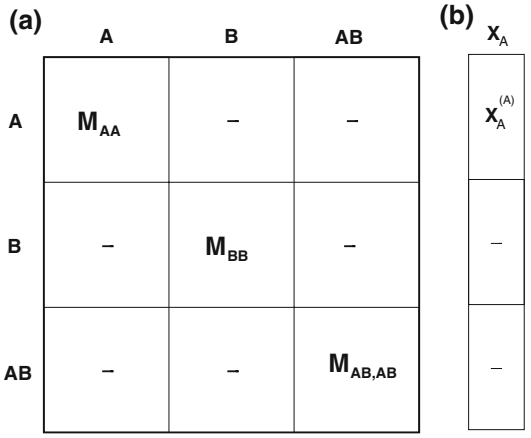

Fig. 8 **a** Block structure of the ADC-ISR secular matrix $\boldsymbol{M}$ with respect the separate fragment model. **b** Structure of ADC-ISR eigenvectors for a local excitation (on fragment A)

6 Concluding remarks

The basic concept underlying the CCLR and EOM-CC methods for electronic excitation in atoms and molecules consists in a specific biorthogonal representation of the (shifted) Hamiltonian in terms of two distinct sets of states: on the one hand, the set of excited CC states based on the CC ground state, and, on the other hand, the set of their biorthogonal counterparts. This results in a non-hermitian (bCC) secular matrix. The excitation energies are obtained as the eigenvalues of the bCC secular matrix, while both the left and right eigenvectors enter the calculation of the spectral intensities. The two sets of states are of quite different quality. While the latter (biorthogonal) basis states are essentially of the CI-type, that is, excited HF configurations, the excited CC states, by contrast, are formed by applying physical excitation operators to the correlated N-electron ground state. The resulting correlated excited (CE) states are expected to be superior to the simple CI states, as they already account for a major part of electron correlation. The intuitive idea here is that electron correlation in excited states should not be completely different from that in the ground state. In fact, the use of CE intermediate states warrants distinctive advantages over the simple CI treatment. Foremost, this concerns the truncation error associated with limited expansion manifolds. To

attain comparable accuracy, the manifold of CE states can be truncated at distinctly smaller excitation levels than the CI expansions. Moreover, the excited CC states are intrinsically separable with regard to (hypothetical) non-interacting fragments, which, in contrast to CI, allows devising size-consistent approximation schemes based on truncated expansion manifolds.

However, due to the equitable use of the biorthogonal set of states being essentially of the CI-type, the bCC representation must be viewed as a CI-ISR hybrid rather than a full ISR approach. This becomes strikingly manifest in the split order structure of the bCC secular matrix, being canonical and of CI-type in the LL and UR parts, respectively. As a result, the truncation error and separability properties are clearly superior to those of CI, but also weaker than those of a full ISR method, such as the ADC-ISR presented in Sect. 5. This is reflected in the general TEO formulas derived here for excitation energies, transition moments and property matrix elements. In the case of single excitations at truncation level 2 (that is, neglecting triply and higher excited configurations), the TEOs in the excitation energies and transition moments are 2, 3 and 4 for CI, bCC and ADC, respectively. At higher truncation levels, the gap between CI and bCC, as well as that between bCC and ADC widens. At the (already somewhat academic) truncation level 6, the respective TEOs are 6, 9 and 12. Of course, a given approximation may not exhaust the margin afforded by the respective TEO. For example, the error in the transition moments of the CC2 scheme is of PT order 2 (due to the first-order approximation used for the T_2 amplitudes), while the truncation error is of PT order 3. The ADC(2) approximation allows for a consistent treatment of (single excitation) energies and transition moments through second order, the TEO being 4. Let us note that the PT order of the overall error is only an indicator for the quality of an approximation scheme. A large error order does not by itself guarantee accurate results, but rather must be seen as a necessary condition for accuracy: a certain accuracy level can only be attained in compliance with a corresponding PT order of the characteristic error.

The hybrid character of the bCC representation is also reflected in the separability properties. The excitation energies, given as the roots of the characteristic polynomial, are separable, which, in principle, ensures size-consistent results at approximative levels beneath the full bCC treatment. It should be noted, however, that the separability of the eigenvalues applies strictly speaking only to the (fictitious) separated fragment model. Allowing for a small interaction between the fragments A and B, which is a more realistic simulation of an extended system, the separability becomes blurred because the coupling block $\boldsymbol{M}_{AB,A}$ (see Fig. 4) no longer vanishes, and local and non-local excitations may mix. What is problematic here is that the small matrix elements of $\boldsymbol{M}_{AB,A}$, associated with the weak physical coupling of the fragments, form products, e.g., in the characteristical polynomial, with the large (non-local coupling) matrix elements of $\boldsymbol{M}_{A,AB}$. The mixing can become substantial when local and non-local excitations are nearly degenerate. This problem has been addressed by Helgaker et al. (see p. 684), but a thorough dedicated study seems to be still pending.

The bCC eigenvectors do not perform uniformly, as the left and right eigenvectors are non-seperable and seperable, respectively. In the associated left and (ordinary) right transition moments, both of which are needed for the computation of spectral intensities, the separability properties are reversed: separable left TMs, as opposed to non-separable right TMs. This reversal is due to the use of the dual ground state and the CC ground state in the right and left TMs, respectively. As a result, the spectral intensities based on the ordinary bCC TMs are not size consistent. This problem does not arise within the CCLR framework, as a separable, though more involved, expression for the right TM is used. In the full bCC limit, the CCLR expression and the ordinary one, used in the EOM-CC methods, are equivalent. At approximate levels, however, the consistency of the left (ordinary) and right (CCLR) TMs may become an issue. At the simple CCS (singles) level, for example, both the left and ordinary right TMs are consistent through zeroth order (due to the use of the HF ground state). The right TM in the CCLR formulation, however, is consistent through first order. This means that the CCLR spectral intensity expression combines a zeroth-order left TM and a first-order right TM. One might be inclined to see this as an improvement, but it should be noted that a result comprising incomplete first-order terms may be inferior to that of a consistent zeroth-order approximation. The consistency problem emerges also in the finding that for transitions with low spectral strengths, the signs of the left and right CCLR transition moments may differ, leading to unphysical (i.e., negative) intensities. This is to say that the CCLR results are not necessarily more accurate than those of EOM-CC as long as size consistency does not play a role. A conclusive comparative test of EOM-CC and CCLR intensity results for smaller and medium-sized molecules would be highly desirable. Such a study should also comprise excited-state properties for which both ordinary non-separable bCC or separable CCLR expressions are available.

Of course, the most obvious drawback of the bCC methods is the non-hermiticity of the respective secular matrices $\boldsymbol{M}$. As already discussed, both the right and left eigenvectors are needed when spectral intensities and property matrix elements are to be determined, which requires an additional

effort compared to the hermitian eigenvalue problem of a full ISR method. In the case of degenerate eigenvalues, care has to be taken to ensure the proper biorthogonalization of the associated sets of left and right eigenvectors. More disturbing is the possibility of complex eigenvalues. Even though the underlying Hamiltonian is hermitian, so that the excitation energies obtained as eigenvalues of $\boldsymbol{M}$ must ultimately (in the full bCC limit) be real quantities, one may encounter problems in actual computations. As first noticed and analyzed by Hättig [35], complex eigenvalues can occur in the vicinity of conical intersections of two excited state energy surfaces (or hyper-surfaces). Köhn and Tajti [36] have developed some ideas on how to deal with that situation, but so far there remain open questions.

The present analysis of the bCC methods for (neutral) electron excitations in an N-electron system can readily be extended to the case of generalized excitations, such as $(N-1)$-or $(N+1)$-electron excitations used in the treatment of ionization or electron attachment processes, respectively. Corresponding CC methods have been referred to as IP-EOM-CC and EA-EOM-CC [37–40]. In the case of (single) ionization, the neutral operators (4) have to be replaced by the manifold

$$\{\hat{C}_J\} \equiv \{c_k; c_a^\dagger c_k c_l, k<l; \ldots\} \tag{142}$$

of physical $1h$-, $2h-1p$-, $3h$-$2p$-,... operators. As in the case of neutral excitations, the successive $(N-1)$-electron excitation classes of μh-$(\mu-1)p$ excitations are labeled by $\mu = 1, 2, \ldots$; a corresponding classification, $[n] = 1, 2, \ldots$, applies to the cationic energy eigenstates $|\Psi_n^{N-1}\rangle$, indicating the respective PT parentage. In the $(N-1)$-electron case (as in the other generalized excitations), the complication arising from an admixture of the N-electron ground state in the neutral excitations (Eqs. 38–41) does not apply, which somewhat simplifies the ionic bCC equations. With a few obvious adjustments, the discussion and the findings for the neutral excitations can readily be transferred to the case of $(N-1)$-electron (and the other generalized) bCC schemes. It should be noted that here generalized transition moments $T_n = \langle\Psi_0|\hat{D}|\Psi_n^{N-1}\rangle$ come into play, defined with respect to a suitable electron removal (or attachment) operator of the type $\hat{D} = \sum_p d_p c_p^\dagger$. This means that in the bCC representation $D_{IJ} = \langle\overline{\Phi}_I|\hat{D}|\Psi_J^0\rangle$ to be used in the analogs of Eqs. 70 and 71, the states $\langle\overline{\Phi}_I|$ on the left side of the matrix elements are the N-electron biorthogonal states (Eq. 16 based on the neutral operators 4). In the discussion of ionic state properties and transition moments according to Sect. 4.5, again a particle-number conserving operator $\hat{D}$ is to be considered. The corresponding bCC representation, $D_{IJ} = \langle\overline{\Phi}_I|\hat{D}|\Psi_J^0\rangle$, is a pure $(N-1)$-electron representation, where both $\langle\overline{\Phi}_I|$ and $|\Psi_J^0\rangle$ are based on the operators (142).

The analysis given here of the EOM-CC and CCLR methods from the perspective of the bCC representation has shown decisive advantages over the conventional CI treatment, but also distinctly weaker TEO and separability properties than those of a full ISR approach such as the ADC-ISR. It should be noted, however, that the latter approach is manifestly based on PT for the secular matrix elements and effective transition coefficients, behaving essentially like the Rayleigh–Schrödinger (RS) PT expansions of the ground-state energies and CI expansion coefficients. This means that the ADC methods and ground-state PT have the same condition of applicability, namely a sufficiently large energy gap between the occupied and virtual HF orbital energies. When the energy gap becomes too small, for example, at bond breaking nuclear conformations, PT based methods are bound to fail. The bCC quantities (secular matrix elements and basis set transition moments), on the other hand, are based on the T-amplitudes of the CC ground state, which can be determined in a completely non-perturbative way. Yet, this edge over methods involving PT must be relativized, as the CC approach breaks down as well in situations where the ground state is no longer adequately described by a dominant single reference configuration (see Bartlett and Musial [41], Sect. 6C, and references therein). The reason is that the usual single-reference CC ansatz is ill suited to deal with the so-called static correlation. As a remedy for this deficiency, much effort has been devoted to developing multi-reference (MR) CC schemes [42–48] (for a more complete list of references and an introduction into the vast field of MRCC methods, the reader is referred to Sect. 9 in the recent review article by Bartlett and Musial [41]). However, the MRCC approach to ground and excited states is far more complex than the single reference bCC representation considered here, and it is to be seen whether really effective computational schemes will emerge.

Acknowledgments JS is indebted to Anthony Dutoi for illuminative discussions on various aspects of the ground-state coupled-cluster method.

Appendix 1: Order relations of bCC representations

A general proof of the canonical order relations in the lower left (LL) triangle of the bCC secular matrix can be found in Ref. [18]. A brief review of the derivation of these order relations is given in the following.

Let us first consider the simpler case of a one-particle operator $\hat{D}$, reading in second-quantized notation

$$\hat{D} = \sum d_{pq} c_p^\dagger c_q \tag{143}$$

where $d_{pq} = \langle\phi_p|\hat{d}|\phi_q\rangle$ denote the one-particle matrix elements associated with $\hat{D}$. The bCC representation of $\hat{D}$,

$$D_{IJ} = \langle \overline{\Phi}_I | \hat{D} | \Psi_J^0 \rangle = \langle \Phi_I | e^{-\hat{T}} \hat{D} e^{\hat{T}} | \Phi_J \rangle \quad (144)$$

was encountered in the treatment of transition moments and excited-state properties, as discussed in Sects. 4.2 and 4.5 (see Eq. 71).

The bCC representation matrix $\boldsymbol{D}$ has an order structure associated with the partitioning according to excitation classes, as shown in Fig. 5. In the upper right (UR) triangle one finds the familiar CI structure for a one-particle operator. This result follows along the lines of the first paragraph in Sect. 4.1. In the lower left (LL) triangle, the canonical order relations

$$D_{IJ} = O([I] - [J] - 1), \quad [I] > [J] \quad (145)$$

apply, which is to be shown in the following.

The operator in the bCC matrix element (144) has a finite Baker–Hausdorff (BH) expansion,

$$e^{-\hat{T}} \hat{D} e^{\hat{T}} = \hat{D} + [\hat{D}, \hat{T}] + \frac{1}{2}[[\hat{D}, \hat{T}], \hat{T}] \quad (146)$$

terminating here already after the double commutator term, because

$$\hat{T} = \sum t_I \hat{C}_I \quad (147)$$

consists of physical excitation operators only, and $\hat{D}$ has at most two unphysical operators. Let us now write the $\hat{T}$ operator according to

$$\hat{T} = \sum \hat{T}_\mu \quad (148)$$

in terms of individual class operators $\hat{T}_\mu, \mu = 1, 2, \ldots$. The T-amplitudes, being themselves subject of a well-defined (diagrammatic) PT, exhibit the order relations (see Hubbard [49])

$$\hat{T}_\mu \sim O(\mu - 1), \quad \mu > 1 \quad (149)$$

This means, for example, that the PT expansions of the T_2 amplitudes

$$\hat{T}_2 = \sum t_{abij} \hat{C}_{abij} \quad (150)$$

begin in first order. The T_1 amplitudes ($\mu = 1$), being of second order, are an exception reflecting Brioullin's theorem.

What are the consequences of the expansion (146) and the order relations (149)? Since the BH expansion (146) begins with $\hat{D}$, there will be non-vanishing zeroth-order contributions to D_{IJ} for $[I] = [J]$ and $[I] = [J] + 1$. Now suppose that I and J differ by more than one class, that is, $[I] \geq [J] + 2$. In that case non-vanishing contributions in D_{IJ} will arise only if there are terms in the BH expansion that are at least of rank $r = [I] - [J]$. Here, the rank of an operator is the number of its $c^\dagger$ (or c) factors. For example, $\hat{D}$ is of rank 1 and the $\hat{T}_\mu$ operators are of rank μ. Now it is readily established that the commutators $[\hat{D}, \hat{T}_\mu]$ and $[[\hat{D}, \hat{T}_\mu], \hat{T}_\nu]$ are of rank μ and $\mu + \nu - 1$, respectively (a commutator of two operators $\hat{A}$ and $\hat{B}$ with definite ranks, a and b, respectively, is of rank $a + b - 1$). To determine the lowest (non-vanishing) PT contribution to the D_{IJ} matrix elements, one has to inspect the terms of the BH expansion (146) having rank $r = [I] - [J]$ (which is the lowest rank allowing for non-vanishing matrix elements) and find the lowest PT order of those terms. For example, $[\hat{D}, \hat{T}_2]$ is of rank 2 and PT order 1, which means that for $[I] = [J] + 2$ the PT order of D_{IJ} is 1. In the general case, $[I] = [J] + \mu$, $\mu \geq 3$, terms with the required rank $r = \mu$ and lowest PT order are due to the $[\hat{D}, \hat{T}_\mu]$ commutators, being of rank μ and PT order $\mu - 1$. Likewise, also the double commutator $[[\hat{D}, \hat{T}_2], \hat{T}_{\mu-1}]$ gives rise to terms with rank μ and order $\mu - 1$, but there are no rank μ terms with PT order lower than $\mu - 1$. This proves the order relations (145).

Let us note that the order relations $\langle \overline{\Phi}_I | \hat{D} | \Psi_0^{\mathrm{cc}} \rangle \sim O([I] - 1)$ for the left basis state transition moments (Eq. 65) follow as special case ($[J] = 0$).

In a similar way, the canonical order relations

$$M_{IJ} = O([I] - [J]), \quad [I] \geq [J] \quad (151)$$

for the bCC secular matrix (LL triangle) elements

$$M_{IJ} = \langle \overline{\Phi}_I | \hat{H} - E_0 | \Psi_J^0 \rangle = \langle \Phi_I | e^{-\hat{T}} [\hat{H}, \hat{C}_J] e^{\hat{T}} | \Phi_0 \rangle \quad (152)$$

can be established. Now, we have to consider the BH expansion involving the commutator $\hat{K}_J = [\hat{H}, \hat{C}_J]$ and check the emerging transition matrix elements of the type $\langle \Phi_I | \hat{O} | \Phi_0 \rangle$. In contrast to the case of the transition operator considered above, $\hat{K}_J$ is itself of PT order 1 and of rank $[J] + 1$ (regarding here only the relevant two-particle part of the Hamiltonian). The BH expansion

$$e^{-\hat{T}} \hat{K}_J e^{\hat{T}} = \hat{K}_J + [\hat{K}_J, \hat{T}] + \frac{1}{2}[[\hat{K}_J, \hat{T}], \hat{T}] + \frac{1}{6}[[[\hat{K}_J, \hat{T}], \hat{T}], \hat{T}] \quad (153)$$

terminates after the triple commutator, since K_J has not more than three unphysical $c^\dagger$ (c) operators. Let us consider a secular matrix element M_{IJ}, where $[I] = [J] + \mu$, $\mu \geq 1$. Obviously, the terms of the BH expansion (153) do not contribute to M_{IJ} if their rank is smaller than $[I]$. As above, we may analyze the terms of rank $r = [J] + \mu$ with respect to their PT order. For $\mu = 1$, the first term $\hat{K}_J$ on the RHS of Eq. 153 is of rank $[J] + 1$ and order 1, thus giving rise to a first-order contribution to M_{IJ}. For higher values of μ, it suffices to consider the commutators $[\hat{K}_J, \hat{T}_\mu]$, being of the required rank $r = [J] + \mu$ and PT order μ. Again, it is readily established that there are no rank $r = [J] + \mu$ terms of lower PT order.

Appendix 2: Order relations of CI and bCC eigenvector matrices

The order structure of the CI and bCC secular matrices give rise to specific order relations for the eigenvector matrices, which, in turn, imply the respective truncation errors in the excitation energies and transition moments. In the following, we will first consider the CI eigenvector matrix, and then turn to the left and right eigenvector matrices associated with the bCC representation. Finally, we shall show how order relations established only for a triangular part of a matrix can be extended to the entire matrix as a consequence of unitarity.

CI eigenvector matrix

The order relations of the CI eigenvector matrix rely on PT for the exact states. Let us first consider the familiar case of the ground state, where the well-known Rayleigh–Schrödinger PT can be cast in the compact form

$$|\Psi_0\rangle = |\Phi_0\rangle + \sum_{v=1}^{\infty}\left[\frac{\hat{Q}_0}{E_0^{(0)} - \hat{H}_0}\left(\hat{H}_I - E_0 + E_0^{(0)}\right)\right]^v |\Phi_0\rangle \tag{154}$$

Here, the usual Møller–Plesset decomposition of the Hamiltonian

$$\hat{H} = \hat{H}_0 + \hat{H}_I \tag{155}$$

into an unperturbed (HF) part $\hat{H}_0$ and an interaction part $\hat{H}_I$ is supposed; $|\Phi_0\rangle$ is the (HF) ground state of $\hat{H}_0$ with the energy $E_0^{(0)}$, and $\hat{Q}_0 = \hat{1} - |\Phi_0\rangle\langle\Phi_0|$. To determine the lowest (nonvanishing) PT order for a specific eigenvalue component,

$$X_{J0} = \langle\Phi_J|\Psi_0\rangle \tag{156}$$

one has to analyze the contributions arising from the expansion on the RHS of Eq. 154. In the vth order, the leading operator term is $\hat{H}_I^v$. Due to the two-electron (Coulomb repulsion) part of $\hat{H}_I$, the matrix element $\langle\Phi_J|\hat{H}_I^v|\Phi_0\rangle$ vanishes if the excitation class of J exceeds the value $2v$. For the excitation classes $[J] = 2v$ and $[J] = 2v - 1$, on the other hand, the matrix element gives rise to a non-vanishing vth order contribution. Obviously, there is no lower-order coupling between the HF ground state and excitations of class $2v$ and $2v - 1$. This means that X_{J0} is of PT order v for $[J] = 2v$ and $[J] = 2v - 1$.

This result can also be written in the form

$$O[\underline{X}_{\mu 0}] = \begin{cases} \frac{1}{2}\mu, & \mu \text{ even} \\ \frac{1}{2}(\mu+1), & \mu \text{ odd}, > 1 \end{cases} \tag{157}$$

where μ denotes collectively the configurations of class μ. The p–h excitation class ($\mu = 1$) is an exception, as here $X_{J0} \sim O(2)$ due to Brioullin's theorem. The ground-state component X_{00} is of course of zeroth order. In Fig. 1, the order structure of $\underline{X}_0$ is depicted.

Now we turn to the order relations of excited states $|\Psi_n\rangle$. Rather than using individual PT expansions, the following analysis will be based directly on the order structure of the CI secular matrix (Fig. 1). However, a remark concerning the significance of excited-state PT is appropriate. As is well known, PT expansions for excited states and excited-state energies are of little practical use because the possibility of small or vanishing denominators ("dangerous denominators") in the PT expansions prevents meaningful computational results. In a formal sense, however, excited-state PT expansions can be generated analogously to the ground-state case, which then can be used to analyze, e.g., truncation errors of excited-state energies and transition moments. Underlying such a formal PT is the concept that each excited state is related to a specific CI state,

$$|\Psi_n\rangle \leftarrow |\Phi_J\rangle,$$

from which it emerges when the scaled interaction, e.g., in the form $\lambda\hat{H}_I$, is gradually increased from $\lambda = 0$ to 1. For our purpose, we do not need the individual PT descent of an exact excited state. It suffices to suppose that the exact states can be classified according to their derivation from the (unperturbed) CI excitation classes, p–h, $2p$–$2h$, ..., etc. Analogously to the notation used for the CI excitation classes, we will denote by $[n]$ the class of the exact state $|\Psi_n\rangle$, that is, $[n] = \mu$ if the excited state n derives from the μp–μh class of CI states. The classification of both the CI and the exact states allows one to partition the CI eigenvector matrix $\boldsymbol{X}$ into sub-blocks $\boldsymbol{X}_{\mu\nu}$, where μ and ν refer to the component and state classes, respectively. Figure 9 shows the partitioning and the associated order structure of $\boldsymbol{X}$. A general expression for the order structure is as follows:

$$O[\boldsymbol{X}_{\mu\nu}] = \begin{cases} \frac{1}{2}|\mu - \nu|, & \mu - \nu \text{ even} \\ \frac{1}{2}|\mu - \nu| + \frac{1}{2}, & \mu - \nu \text{ odd} \end{cases} \tag{158}$$

The order relations of the eigenvector matrix reflect the underlying order structure of the CI secular matrix. We begin by considering the class of singly excited states ($[n] = 1$). Rather than dealing with individual eigenvectors, we can treat the entire set of class-1 eigenvectors at the same time. Let us therefore denote by $\underline{\boldsymbol{X}}_1$ the rectangular matrix formed by all (column) eigenvectors $\underline{X}_n$ with $[n] = 1$. The eigenvalue equations for the eigenvectors of class 1 can be written compactly as

$$\boldsymbol{H}\underline{\boldsymbol{X}}_1 = \underline{\boldsymbol{X}}_1\boldsymbol{\Omega}_1 \tag{159}$$

where $\boldsymbol{\Omega}_1$ denotes the diagonal matrix of the p–h energy eigenvalues. Since any eigenvalue ω_n has an orbital energy

	1	2	3	4	5	6	⋯
1	0	1	1	2	2	3	
2	1	0	1	1	2	2	
3	1	1	0	1	1	2	
4	2	1	1	0	1	1	
5	2	2	1	1	0	1	
6	3	2	2	1	1	0	
⋮							

Fig. 9 Order relations of the CI eigenvector matrix $\boldsymbol{X}$. Block structure and entries as in Figs. 1 and 3

(zeroth order) contribution, that is, $\boldsymbol{\Omega}_1 \sim O(0)$, Eq. 159 leads to the following order equation

$$O[\boldsymbol{H}\underline{\boldsymbol{X}}_1] = O[\underline{\boldsymbol{X}}_1] \tag{160}$$

This equation can be used to establish successively the individual orders of the component blocks, $\boldsymbol{X}_{k,1}$. Obviously, the starting point is given by $\boldsymbol{X}_{1,1} \sim \mathbf{1} + O(1)$, which merely reflects the fact that the singly excited states derive from the p–h CI configurations. To proceed, we inspect the matrix–vector block products $\sum_j \boldsymbol{H}_{k,j}\ \boldsymbol{X}_{j,1}$ for successive values of the (row) index k. (to visualize these products, it is helpful to write the order structure of $\boldsymbol{H}$ (Fig. 1) alongside the $\underline{\boldsymbol{X}}_1$ column matrix and fill in the successively determined order entries here, starting with the entry 0 in the $\boldsymbol{X}_{1,1}$ sub-block). For $k = 2$ we may readily conclude that

$$\boldsymbol{X}_{2,1} \sim \sum_{j \geq 1} \boldsymbol{H}_{2,j}\boldsymbol{X}_{j,1} \sim O(1) \tag{161}$$

where the first-order behavior comes from the first term in the sum, $\boldsymbol{H}_{2,1}\,\boldsymbol{X}_{1,1} \sim \boldsymbol{H}_{2,1} \sim O(1)$. [Note that the diagonal eigenvector block behaves as $\boldsymbol{X}_{1,1} = \mathbf{1} + O(1)$]. In a similar way, we may establish that also the next sub-block is of first order, $\underline{\boldsymbol{X}}_{3,1} \sim O(1)$. For the fourth sub-block, the situation changes since the $\boldsymbol{H}_{4,1}$ matrix block vanishes so that here and beyond the zeroth-order $\boldsymbol{X}_{1,1}$ block drops out. One here obtains

$$\underline{\boldsymbol{X}}_{4,1} \sim \sum_{j \geq 2} \boldsymbol{H}_{4,j}\boldsymbol{X}_{j,1} \sim O(2) \tag{162}$$

where the second-order behavior of $\boldsymbol{X}_{4,1}$ derives from the first two summands involving the two first-order sub-blocks $\boldsymbol{X}_{2,1}$ and $\boldsymbol{X}_{3,1}$. In the next step, one first-order block drops out of the matrix–vector product, but the second one, $\boldsymbol{X}_{3,1}$, combined with the $\boldsymbol{H}_{5,3}$ block of the secular matrix, again leads to second-order behavior of $\boldsymbol{X}_{5,1}$. Only for $k = 6$ the order jumps to 3, since now due to the structure of the secular matrix, the first-order blocks (and the zeroth-order block) no longer contribute to the matrix–vector product. Continuing in this way, the order relations of successively higher-class sub-blocks can be obtained. The general pattern is that for each even k, the order of the $\boldsymbol{X}_{k,1}$ block increases by 1. Let us note that the procedure can readily be cast in the formally correct form of induction.

Now, we may proceed to the next higher class of $2p$–$2h$ states. Let $\underline{\boldsymbol{X}}_2$ denote the $2p$–$2h$ eigenvector matrix with the (sub)blocks $\boldsymbol{X}_{k,2}$. In accord with the PT origin of the $2p$–$2h$ states, here the $k = 2$ (diagonal) block is of zeroth order, more specifically, $\boldsymbol{X}_{2,2} \sim \mathbf{1} + O(1)$. But the order of the first block, $\boldsymbol{X}_{1,2}$ is fixed as well. As will be demonstrated below (Order relations for biorthogonal matrices), the orthogonality of the p–h and $2p$–$2h$ eigenvectors requires that $\boldsymbol{X}_{1,2}$ is of first order. In a similar way as above, the orders of the higher k blocks can now be derived successively from the matrix–vector products

$$\boldsymbol{X}_{k,2} \sim \sum_{j \geq 1} \boldsymbol{H}_{k,j}\boldsymbol{X}_{j,2} \tag{163}$$

It is readily established that the $\boldsymbol{X}_{3,2}$ and $\boldsymbol{X}_{4,2}$ blocks are of first order, followed by two blocks of second order and so forth.

The procedure outlined here for the p–h and $2p$–$2h$ states can easily be extended to higher excitation classes, μ. The diagonal block, $\boldsymbol{X}_{\mu,\mu} \sim \mathbf{1} + O(1)$ is always of zeroth order, while the order relations for blocks above the diagonal, $k < \mu$, are determined by the orthogonality between the eigenvectors of class μ and those of the lower classes [see below: Order relations for biorthogonal matrices]. In the $3p$–$3h$ states, for example, the orthogonality constraint with respect to the p–h and $2p$–$2h$ states requires the $\boldsymbol{X}_{1,3}$ and $\boldsymbol{X}_{2,3}$ blocks to be of first order. The full procedure for establishing the order relations of $\boldsymbol{X}$, ascending both to higher excitation classes and higher blocks within a given excitation class, can, of course, be reformulated in a formally satisfactory way making use of induction.

Once the order structure of the eigenvectors has been established, it is straightforward to analyze the truncation errors of the excitation energies. For this purpose, one has to express an eigenvalue according to

$$E_n = \underline{X}_n^{\dagger}\boldsymbol{H}\underline{X}_n \tag{164}$$

as an energy expectation value, involving the full secular matrix $\boldsymbol{H}$ and the exact eigenvector $\underline{X}_n$. This expectation value can be written more explicitly as

$$E_n = \sum_{\kappa,\lambda} \underline{X}_{\kappa n}^{\dagger}\boldsymbol{H}_{\kappa,\lambda}\underline{X}_{\lambda n} \tag{165}$$

where the Greek subscripts refer to excitation classes rather than to individual configurations. To specify the error

arising from truncating the CI manifold after class μ, one has to inspect the PT order of the terms with $\kappa = \mu + 1$, $\lambda \leq \mu + 1$ (or $\lambda = \mu + 1$, $\kappa \leq \mu + 1$). Due to the structure of $\boldsymbol{H}$, it suffices to consider the diagonal contribution $\underline{X}^{\dagger}_{\mu+1,n}\boldsymbol{H}_{\mu+1,\mu+1}\underline{X}_{\mu+1,n}$ Since $\boldsymbol{H}_{\mu+1,\mu+1} \sim O(0)$, the latter term is of the order

$$O[\underline{X}^{\dagger}_{\mu+1,n}\underline{X}_{\mu+1,n}] = 2O[\underline{X}_{\mu+1,n}] \tag{166}$$

Using Eq. 158, this translates into the general truncation error formula

$$O^{[n]}_{\mathrm{TE}}(\mu) = \begin{cases} \mu - [n] + 2, & \mu - [n] \text{ even} \\ \mu - [n] + 1, & \mu - [n] \text{ odd} \end{cases} \tag{167}$$

for the CI excitation energies of class $[n]$, where, of course, $\mu \geq [n]$ is supposed. In a similar way, one may analyze the expression (9) for the transition moments, yielding the following truncation error formula:

$$O^{[n]}_{\mathrm{TE}}(\mu) = \begin{cases} \mu - \frac{1}{2}[n] + 1, & [n] \text{ even} \\ \mu - \frac{1}{2}[n] + \frac{1}{2}, & [n] \text{ odd} \end{cases} \tag{168}$$

Note that for the case of single excitations, $[n] = 1$, the general formulas (167, 168) reduce to the simple expressions (7) and (11), respectively, given in Sect. 2.

For completeness, let us note that the simple expression

$$O^{[n]}_{\mathrm{TE}}(\mu) = \mu - [n] + 1 \tag{169}$$

applies to the truncation error of property matrix elements

$$T_{nn} = \underline{X}^{\dagger}_{n}\boldsymbol{D}\underline{X}_{n} \tag{170}$$

Here, $\boldsymbol{D}$ is the CI representation (10) of a one-particle operator.

bCC eigenvector matrices

The order structures of the right and left bCC eigenvector matrices $\boldsymbol{X}$ and $\boldsymbol{Y}$, respectively, are shown in Fig. 10. Note that $\boldsymbol{X}$ now denotes the right bCC eigenvector matrix rather than the CI eigenvector matrix as above (CI eigenvector matrix). The bCC eigenvector matrices display both canonical and CI-type order structures. The LL part of $\boldsymbol{X}$ and the UR part of $\boldsymbol{Y}$ are canonical,

$$O[\boldsymbol{X}_{\mu\nu}] = O[\boldsymbol{Y}_{\nu\mu}] = \mu - \nu, \quad \mu \geq \nu \tag{171}$$

while the UR part of $\boldsymbol{X}$ and the LL part of $\boldsymbol{Y}$ are of CI-type,

$$O[\boldsymbol{X}_{\nu\mu}] = O[\boldsymbol{Y}_{\mu\nu}] = \begin{cases} \frac{1}{2}(\mu - \nu), & \mu - \nu \text{ even}, \geq 0 \\ \frac{1}{2}(\mu - \nu) + \frac{1}{2}, & \mu - \nu \text{ odd}, \geq 0 \end{cases} \tag{172}$$

The order structures of the bCC eigenvector matrices can be deduced from the order structure of the bCC secular matrix by an obvious generalization of the procedure used above for the CI eigenvector matrix. Here, it is important that at each successive step associated with an excitation class μ, both the right and left eigenvector matrices $\underline{\boldsymbol{X}}_{\mu}$ and $\underline{\boldsymbol{Y}}_{\mu}$ must be treated in parallel, while the biorthogonality to the respective eigenvectors of the lower excitation classes, $1, \ldots, \mu - 1$, must successively be taken into account. A formally correct way of translating the structure of the bCC secular matrix into the order structures of the eigenvector matrices can readily be spelled out.

However, one may take also an alternative route, in which the order structures of the UR parts of both $\boldsymbol{X}$ and $\boldsymbol{Y}$ are determined directly. The order relations of the complementary LL parts are then obtained as a result of the biorthogonality, $\boldsymbol{Y}^{\dagger}\boldsymbol{X} = \boldsymbol{1}$. Let us first consider an eigenvector component

$$X_{Jn} = \langle\overline{\Phi}_J|\Psi^{(r)}_n\rangle, \quad [n] \geq [J] \tag{173}$$

from a UR block of $\boldsymbol{X}$. Since $|\Psi^{(r)}_n\rangle$ differs from the (normalized) exact eigenstate $|\Psi_n\rangle$ only by a normalization constant ($N_n \sim 1 + O(2)$), we may consider $\langle\overline{\Phi}_J|\Psi_n\rangle$ rather than X_{Jn}, that is,

$$X_{Jn} \sim \langle\overline{\Phi}_J|\Psi_n\rangle \tag{174}$$

Using the expansion (30) for $\langle\overline{\Phi}_J|$, it is apparent that for $[n] \geq [J]$ the bCC eigenvecor component is of the same order as the corresponding CI eigenvector component:

$$O[\langle\overline{\Phi}_J|\Psi_n\rangle] = O[\langle\Phi_J|\Psi_n\rangle] \tag{175}$$

This establishes the CI-type order relations for the UR part of $\boldsymbol{X}$.

In analogy to Eq. 174, the left bCC eigenvector components,

$$Y_{Jn} = \langle\Psi^{(l)}_n|\Psi^0_J\rangle \tag{176}$$

can be related to the normalized eigenstates,

$$Y_{Jn} \sim \langle\Psi_n|\Psi^0_J\rangle = \langle\Psi_n|\hat{C}_J|\Psi^{\mathrm{cc}}_0\rangle \sim \langle\Psi_n|\hat{C}_J|\Psi_0\rangle \tag{177}$$

where we have used the fact that the CC and the normalized ground state differ by a normalization constant of the order $1 + O(2)$. So it remains to show the order relations

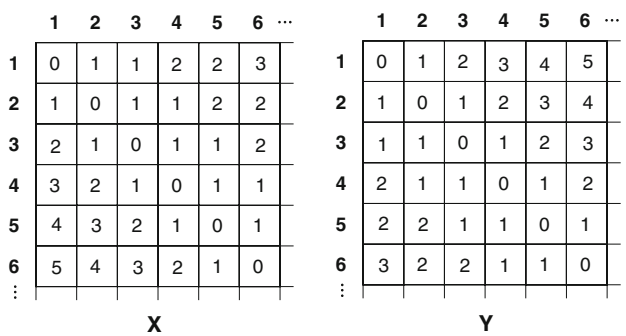

Fig. 10 Order relations of the right and left bCC eigenvector matrices $\boldsymbol{X}$ and $\boldsymbol{Y}$, respectively. Block structure and entries as in Figs. 1 and 3

$$\langle\Psi_n|\hat{C}_J|\Psi_0\rangle \sim O([n]-[J]), \quad [n]\geq[J] \tag{178}$$

for the "generalized transition moments" (GTM) $\langle\Psi_n|\hat{C}_J|\Psi_0\rangle$. Let us first note that these GTM order relations are non-trivial. For a triply excited state ($[n] = 3$) and a p–h excitation operator ($[J] = 1$), for example, the (canonical) order is 2, rather than 1, as one might expect in view of two individual first-order contributions associated with $|\Psi_n^{(1)}\rangle$ and $|\Psi_0^{(1)}\rangle$, respectively. It is instructive to verify that these two first-order contributions, in fact, cancel each other.

To prove the GTM order relations we may rely on the canonical order relations

$$\langle\Psi_n|\tilde{\Psi}_J\rangle \sim O(|[n]-[J]|) \tag{179}$$

as established for the ISR eigenvector components (see Eq. 132) discussed in Sect. 5. Since the intermediate states $|\tilde{\Psi}_K\rangle$ (including $|\Psi_0\rangle$) form a complete and orthonormal set of states, they can be used to expand the GTM $\langle\Psi_n|\hat{C}_J|\Psi_0\rangle$ as follows:

$$\begin{aligned}\langle\Psi_n|\hat{C}_J|\Psi_0\rangle &= \sum_K \langle\Psi_n|\tilde{\Psi}_K\rangle\langle\tilde{\Psi}_K|\hat{C}_J|\Psi_0\rangle \\ &= \sum_{[K]\leq[J]} \langle\Psi_n|\tilde{\Psi}_K\rangle\langle\tilde{\Psi}_K|\hat{C}_J|\Psi_0\rangle\end{aligned} \tag{180}$$

where the second line is due to the fact that by construction the intermediate states $|\tilde{\Psi}_K\rangle$ are orthogonal to all states $\hat{C}_J|\Psi_0\rangle$ with $[J] < [K]$, that is, $\langle\tilde{\Psi}_K|\hat{C}_J|\Psi_0\rangle = 0$ for $[J] < [K]$. Now for $[n] > [J]$, the order of $\langle\Psi_n|\tilde{\Psi}_K\rangle$ decreases with increasing $[K]$ and so does the order of $\langle\tilde{\Psi}_K|\hat{C}_J|\Psi_0\rangle$. This means that the minimal order contributions in the sum on the RHS of Eq. 180 are due to those where $[K] = [J]$:

$$\langle\Psi_n|\hat{C}_J|\Psi_0\rangle \sim O[\langle\Psi_n|\tilde{\Psi}_J\rangle\langle\tilde{\Psi}_J|\hat{C}_J|\Psi_0\rangle] = O[\langle\Psi_n|\tilde{\Psi}_J\rangle] \tag{181}$$

The last equality follows from the observation that $\langle\tilde{\Psi}_J|\hat{C}_J|\Psi_0\rangle$ is of zeroth order. This completes the proof of the canonical order relations for the eigenvector components in the UR blocks of $\boldsymbol{Y}$.

The biorthogonality of the left and right bCC eigenvector matrices exacts the order relations of the LL blocks of the $\boldsymbol{X}$ and $\boldsymbol{Y}$ matrices, as will be shown below (Order relations for biorthogonal matrices).

Like in the last paragraph of the first subsection (CI eigenvector matrix), the truncation error of the bCC excitation energies for general excitation classes $[n]$ can be deduced from the eigenstate order relations. The starting point is the expression

$$E_n = \underline{Y}_n^\dagger \boldsymbol{M} \underline{X}_n = \sum_{\kappa,\lambda} \underline{Y}_{\kappa n}^\dagger \boldsymbol{M}_{\kappa,\lambda} \underline{X}_{\lambda n} \tag{182}$$

where, analogously to Eq. 165, the second equation reflects the partitioning of the energy expectation value with respect to excitation classes. To determine the TEO at a given truncation level μ, one has to analyze the contributions where $\kappa = \mu + 1$, $[n] \leq \lambda \leq \mu + 1$ (set S_1) and $\lambda = \mu + 1$, $[n] \leq \kappa \leq \mu$ (set S_2). Here, $\mu \geq [n]$ is supposed. The former set of contributions is given by

$$S_1 = \underline{Y}_{\mu+1,n}^\dagger \sum_{\lambda=[n]}^{\mu+1} \boldsymbol{M}_{\mu+1,\lambda} \underline{X}_{\lambda n} \tag{183}$$

Due to the order relations in the LL parts of $\boldsymbol{X}$ (Eq. 171) and $\boldsymbol{M}$ (Eq. 52), we find

$$O[\boldsymbol{M}_{\mu+1,\lambda}\underline{X}_{\lambda n}] = \mu - [n] + 1 \tag{184}$$

irrespective of λ. Together with the OR of $\underline{Y}_{\mu+1,n}$ (Eq. 172), this leads to the following TEO formula

$$O_{\mathrm{TE}}^{[n]}(\mu) = \begin{cases} \frac{3}{2}(\mu-[n])+2, & \mu-[n] \text{ even} \\ \frac{3}{2}(\mu-[n])+\frac{3}{2}, & \mu-[n] \text{ odd} \end{cases} \tag{185}$$

The S_2 set consists only of two contributions,

$$S_2 = \underline{Y}_{\mu,n}^\dagger \boldsymbol{M}_{\mu,\mu+1} \underline{X}_{\mu+1,n} + \underline{Y}_{\mu-1,n}^\dagger \boldsymbol{M}_{\mu-1,\mu+1} \underline{X}_{\mu+1,n} \tag{186}$$

because $\boldsymbol{M}_{\kappa,\mu+1} = \boldsymbol{0}$ for $\kappa < \mu - 1$. The two involved sub-blocks of $\boldsymbol{M}$ are of first order, $O[\boldsymbol{M}_{\mu,\mu+1}] = O[\boldsymbol{M}_{\mu-1,\mu+1}] = 1$, and the TEOs of the S_2 contributions are seen to exceed those of S_1. This means that Eq. 185 is the final expression for the truncation errors in the bCC excitation energies.

In a similar way, one can derive general TEO formulas for the left and right transition moments and the excited-state properties. In case of the right transition moments, the dual ground-state eigenvector $\underline{Y}_0$ comes into play. The CI-type order relations of $\underline{Y}_0$ (see Fig. 3b) can readily be established by analyzing the eigenvalue equation $\underline{Y}_0^\dagger \boldsymbol{M} = -\underline{v}^\mathrm{t}$ (Eq. 34) in a similar way as in the first subsection (CI eigenvector matrix), but assuming that only the p–h and $2p$–$2h$ components of $\underline{v}^\mathrm{t}$ are non-vanishing, the latter being of first order. As expected, both the dual and the CI ground-state have the same order relations, as specified by Eq. 157.

The resulting TEO formulas are as follows.

(i) *left transition moments:*

$$O_{\mathrm{TE}}^{[n]}(\mu) = \begin{cases} \frac{3}{2}\mu - \frac{1}{2}[n], & \mu-[n] \text{ even} \\ \frac{3}{2}\mu - \frac{1}{2}[n] + \frac{1}{2}, & \mu-[n] \text{ odd} \end{cases} \tag{187}$$

(ii) *right transition moments:*

$$O_{\mathrm{TE}}^{[n]}(\mu) = \begin{cases} \frac{3}{2}\mu - [n] + 1, & \mu \text{ even} \\ \frac{3}{2}\mu - [n] + \frac{1}{2}, & \mu \text{ odd} \end{cases} \tag{188}$$

(iii) *property matrix elements:*

$$O_{\mathrm{TE}}^{[n]}(\mu) = \begin{cases} \frac{3}{2}(\mu-[n])+1, & \mu-[n] \text{ even} \\ \frac{3}{2}(\mu-[n])+\frac{1}{2}, & \mu-[n] \text{ odd} \end{cases} \tag{189}$$

As above, $[n]$ and μ denote the final state excitation class and the truncation level, respectively, where of course $\mu \geq [n]$.

The first expression (*i*) is obtained by generalizing the derivation of Eq. 67 in Sect. 4.2. Here the error associated with the truncation of the excited state manifold follows from Eq. 64, using the order relations (66) of the left basis set transition moments together with the CI-type order relations (Eq. 172) in the LL block of the left eigenvector matrix. In addition, one has to account for the error arising from the truncation of the ground-state CC expansion, assuming here the same truncation levels in the ground and excited states. Supposing a sufficiently large or even complete ground-state CC expansion, the TEO increases by 1 for even values of $\mu - [n]$ (first line on the RHS of Eq. 187).

In the case of the right transition moments (*ii*), the TEOs are determined by the second term on the RHS of Eq. 70. This term can be analyzed in an analogous way as the bCC eigenvalues by using the bCC order relations of the transition operator matrix $\boldsymbol{D}$ given in Fig. 5a, rather than those of the bCC secular matrix. It should be noted that apart from the case of single excitations, $[n] = 1$, the right transition moments have larger truncation errors (lower orders) than the left ones.

In (*iii*), finally, one has to analyze the vector × matrix × vector product in Eq. 100. The order relations that come into play are those of $\boldsymbol{D}$ (Fig. 5a) and the LL parts of the left and right eigenvector matrices. It should be noted that the expression (*iii*) applies also to inter-state transition moments for excited states of the same class, $[n] = [m]$.

In the latter two cases, there is each an additional contribution, arising from the admixture of the ground state in the right eigenstate expansion (Eq. 41), specified by the respective (extended) eigenvector component $x_n = -\underline{Y}_0^\dagger \underline{X}_n$ (Eq. 40). Using the order relations for $\underline{Y}_0^\dagger$ and the LL part of the right eigenvector matrix, one can readily derive the following TEO formula for the x_n components:

$$O_{\mathrm{TE}}^{[n]}(\mu) = \begin{cases} \frac{3}{2}\mu - [n] + 2, & \mu \text{ even} \\ \frac{3}{2}\mu - [n] + \frac{3}{2}, & \mu \text{ odd} \end{cases} \tag{190}$$

As discussed in Sects. 4.2 and 4.5, the TEOs in the additional (ground-state admixture) terms exceed those of the respective main contribution.

Order relations for biorthogonal matrices

In the preceding subsection (bCC eigenvector matrices), the order relations for the bCC eigenvector matrices have been established only for the respective UR blocks, being of CI-type in $\boldsymbol{X}$ and canonical in $\boldsymbol{Y}$. Now we will show that the biorthogonality of $\boldsymbol{X}$ and $\boldsymbol{Y}$ requires canonical and CI-type behavior in the LL blocks of $\boldsymbol{X}$ and $\boldsymbol{Y}$, respectively.

Let us first note that the biorthogonality relation

$$\boldsymbol{Y}^\dagger \boldsymbol{X} = \mathbf{1} \tag{191}$$

also implies that

$$\boldsymbol{X}\boldsymbol{Y}^\dagger = \mathbf{1} \tag{192}$$

which will be our starting point here. In this form, the UR order relations of the first factor $\boldsymbol{X}$ (CI-type) match the LL order relations of the second factor $\boldsymbol{Y}^\dagger$ (canonical), which for brevity will be denoted by $\boldsymbol{Y}'$ henceforth. For a graphical notion of the following procedure, we recommend to place the $\boldsymbol{X}$ and $\boldsymbol{Y}'$ partitioning schemes next to each other and fill in successively the emerging order relation entries.

For the first row of $\boldsymbol{X}$-blocks, $\boldsymbol{X}_{1,k}$, $k = 1,2,...$, and the first column of $\boldsymbol{Y}'$-blocks, $\boldsymbol{Y}'_{k,1}$, $k = 1,2,...$, the order relations are already given. In the second row of $\boldsymbol{X}$-blocks and the second column of $\boldsymbol{Y}'$-blocks, there is one undetermined block each, namely, $\boldsymbol{X}_{2,1}$ and $\boldsymbol{Y}'_{1,2}$, respectively. The orthogonality of the second $\boldsymbol{X}$ row and the first $\boldsymbol{Y}'$ column can be expressed as follows:

$$\sum_k \boldsymbol{X}_{2,k}\boldsymbol{Y}'_{k,1} = \mathbf{0} \tag{193}$$

What can be concluded from this with respect to the order of $\boldsymbol{X}_{2,1}$? Let us focus on the first two terms in the sum, the remainder being (at least) of the order 2:

$$\boldsymbol{X}_{2,1}\boldsymbol{Y}'_{1,1} + \boldsymbol{X}_{2,2}\boldsymbol{Y}'_{2,1} + O(2) = \mathbf{0} \tag{194}$$

Since the diagonal blocks of the eigenvector matrices behave as $\boldsymbol{Y}'_{1,1} = \mathbf{1} + O(1)$ and $\boldsymbol{X}_{2,2} = \mathbf{1} + O(1)$, respectively, and $\boldsymbol{Y}'_{2,1} \sim O(1)$, the following relation holds through first order:

$$\boldsymbol{X}_{2,1} + O(1) = \mathbf{0} \tag{195}$$

This means that $\boldsymbol{X}_{2,1}$ must cancel a (non-vanishing) first-order contribution and, thus, is itself of the first order (more accurately, the lowest non-vanishing contribution in the PT expansion of $\boldsymbol{X}_{2,1}$ is of first order). In a similar way, we may conclude $\boldsymbol{Y}'_{1,2} \sim O(1)$, being a consequence of the orthogonality of the second column of $\boldsymbol{Y}'$-blocks and the first row of $\boldsymbol{X}$-blocks.

After having completed the order relations in the second row and column of $\boldsymbol{X}$ and $\boldsymbol{Y}'$, respectively, we may proceed to the third row of $\boldsymbol{X}$-blocks. Here, the orders of the first two blocks, $\boldsymbol{X}_{3,1}$ and $\boldsymbol{X}_{3,2}$, have to be derived, which in turn can be achieved by exploiting that this row is orthogonal to both the first and second column of $\boldsymbol{Y}'$-blocks. Expanded explicitely through the first three terms, these order relations are:

$$\boldsymbol{X}_{3,1}\boldsymbol{Y}'_{1,1} + \boldsymbol{X}_{3,2}\boldsymbol{Y}'_{2,1} + \boldsymbol{X}_{3,3}\boldsymbol{Y}'_{3,1} + O(4) = \mathbf{0} \tag{196}$$

$$\boldsymbol{X}_{3,1}\boldsymbol{Y}'_{1,2} + \boldsymbol{X}_{3,2}\boldsymbol{Y}'_{2,2} + \boldsymbol{X}_{3,3}\boldsymbol{Y}'_{3,2} + O(3) = \mathbf{0} \tag{197}$$

The second equation allows us to determine the order of $\boldsymbol{X}_{3,2}$. Using $\boldsymbol{Y}'_{1,2} \sim O(1)$, $\boldsymbol{Y}'_{3,2} \sim O(1)$, and $\boldsymbol{Y}'_{2,2} = \mathbf{1} + O(1)$,

$\boldsymbol{X}_{3,3} = \mathbf{1} + O(1)$ (as diagonal eigenvector blocks), we may conclude that the relation

$$\boldsymbol{X}_{3,2} + O(1) = \mathbf{0} \tag{198}$$

holds through first order, which, as above, implies that $\boldsymbol{X}_{3,2}$ is of first order. Using this result in the first orthogonality equation, together with $\boldsymbol{Y}'_{1,1} = \mathbf{1} + O(1)$, $\boldsymbol{Y}'_{2,1} \sim O(1)$, and $\boldsymbol{Y}'_{3,1} \sim O(2)$, yields through second order

$$\boldsymbol{X}_{3,1} + O(2) = \mathbf{0} \tag{199}$$

which means that $\boldsymbol{X}_{3,1} \sim O(2)$, consistent with the canonical order relations. In a completely analogous way, the first two blocks in the third column of $\boldsymbol{Y}'$-blocks can be treated, yielding the expected CI-type order results, $\boldsymbol{Y}'_{1,3} \sim O(1)$, $\boldsymbol{Y}'_{2,3} \sim O(1)$.

This brief demonstration shows how the given CI-type UR order relations of $\boldsymbol{X}$ and the canonical LL order relations of $\boldsymbol{Y}'$ ($= \boldsymbol{Y}^{\dagger}$) impose canonical order relations in the LL part of $\boldsymbol{X}$ and CI-type order relations in the UR part $\boldsymbol{Y}^{\dagger}$ as a result of the biorthogonality of right and left bCC eigenvector matrices. Of course, this derivation can readily be cast into a formally correct proof by induction (see Ref. [18]).

In a related way, the unitarity of the CI eigenvector matrix (denoted $\boldsymbol{X}$ in the first subsection, CI eigenvector matrix) can be used to extend the CI order relations (157), established in the first subsection (CI eigenvector matrix) only for the LL part, to the entire matrix $\boldsymbol{X}$. Writing the unitarity relation of the CI eigenvector matrix in the form $\boldsymbol{X}^{\dagger}\boldsymbol{X} = \mathbf{1}$, the order relations of the UR part of $\boldsymbol{X}^{\dagger}$ combine with those of the LL part of $\boldsymbol{X}$, similar to the product (192) of the bCC eigenvector matrices. The successive construction of the CI order relations in the UR part of $\boldsymbol{X}$ can be performed essentially as in the bCC case above.

Appendix 3: Equivalence of CCLR and ordinary bCC transition moments

Right transition moments

In the exact (full) bCC treatment, the ordinary right bCC transition moment (Eq. 46)

$$T_n^{(r)} = \langle \overline{\Psi}_0 | \hat{D}\hat{C}_n | \Psi_0^{cc} \rangle + x_n \langle \overline{\Psi}_0 | \hat{D} | \Psi_0^{cc} \rangle \tag{200}$$

and the separable CCLR expression (Eq. 97)

$$T_n^{(r)} = \langle \overline{\Psi}_0 | [\hat{D}, \hat{C}_n] | \Psi_0^{cc} \rangle - \sum_{I,J} \langle \overline{\Psi}_0 | [[\hat{H}, \hat{C}_I], \hat{C}_n] | \Psi_0^{cc} \rangle \times (\boldsymbol{M} + \omega_n)^{-1}_{IJ} \langle \overline{\Phi}_J | \hat{D} | \Psi_0^{cc} \rangle \tag{201}$$

are equivalent. Here, as in Sect. 4.4,

$$\hat{C}_n = \sum X_{In} \hat{C}_I \tag{202}$$

denotes the (right) excitation operator associated with the nth excited state, $|\Psi_n^{(r)}\rangle = x_n |\Psi_0^{cc}\rangle + \hat{C}_n |\Psi_0^{cc}\rangle$. This by no means obvious result was shown explicitly by Koch et al. [19]. The following is essentially a reformulation and slight extension of the original proof, using the more transparent wave function notations adopted here.

Let us start from the the ordinary bCC expression (200) and transform it successively into the CCLR expression (201). As a first step we make use of the commutator relation $\hat{D}\hat{C}_n = [\hat{D}, \hat{C}_n] + \hat{C}_n\hat{D}$, yielding

$$T_n^{(r)} = \langle \overline{\Psi}_0 | [\hat{D}, \hat{C}_n] | \Psi_0^{cc} \rangle + \langle \overline{\Psi}_0 | \hat{C}_n \hat{D} | \Psi_0^{cc} \rangle + x_n \langle \overline{\Psi}_0 | \hat{D} | \Psi_0^{cc} \rangle \tag{203}$$

To proceed, let us consider the (trivial) identity

$$\langle \overline{\Psi}_0 | \hat{C}_n \hat{D} | \Psi_0^{cc} \rangle = \langle \overline{\Psi}_0 | \hat{C}_n (\hat{H} - E_0 + \omega_n)(\hat{H} - E_0 + \omega_n)^{-1} \hat{D} | \Psi_0^{cc} \rangle \tag{204}$$

and replace the inverse matrix operator on the RHS by its bCC representation. Noting that $\boldsymbol{M}' + \omega_n$ is the bCC representation of $\hat{H} - E_0 + \omega_n$, where $\boldsymbol{M}'$ is the extended bCC secular matrix given by Eq. 27, the bCC representation of the inverse operator reads

$$(\boldsymbol{M}' + \omega_n)^{-1} = \begin{pmatrix} \omega_n^{-1} & \underline{w}_n^t \\ \underline{0} & (\boldsymbol{M} + \omega_n)^{-1} \end{pmatrix} \tag{205}$$

where

$$\underline{w}_n^t = -\omega_n^{-1} \underline{v}^t (\boldsymbol{M} + \omega_n)^{-1} \tag{206}$$

This means that we can express $(\hat{H} - E_0 + \omega_n)^{-1}$ as follows:

$$(\hat{H} - E_0 + \omega_n)^{-1} = \sum_{I,J} |\Psi_I^0\rangle (\boldsymbol{M} + \omega_n)^{-1}_{IJ} \langle \overline{\Phi}_J | + \sum_J w_{nJ} |\Psi_0^{cc}\rangle \langle \overline{\Phi}_J | + \omega_n^{-1} |\Psi_0^{cc}\rangle \langle \Phi_0 |$$

Inserting this expansion into Eq. 204 yields

$$\langle \overline{\Psi}_0 | \hat{C}_n \hat{D} | \Psi_0^{cc} \rangle = \langle \overline{\Psi}_0 | \hat{C}_n (\hat{H} - E_0 + \omega_n) | \Psi_I^0 \rangle (\boldsymbol{M} + \omega_n)^{-1}_{IJ} \langle \overline{\Phi}_J | \hat{D} | \Psi_0^{cc} \rangle - x_n \left\{ \langle \Phi_0 | \hat{D} | \Psi_0^{cc} \rangle + \sum_J \omega_n w_{nJ} \langle \overline{\Phi}_J | \hat{D} | \Psi_0^{cc} \rangle \right\} \tag{207}$$

In deriving this result we have used that $(\hat{H} - E_0 + \omega_n)|\Psi_0^{cc}\rangle = \omega_n |\Psi_0^{cc}\rangle$ and $\langle \overline{\Psi}_0 | \hat{C}_n | \Psi_0^{cc} \rangle = -x_n$. Note that at this point, another x_n-term comes into play, augmenting the third term on the RHS of Eq. 203. The reformulation of Eq. 204 is still not complete. To proceed, the matrix elements $\langle \overline{\Psi}_0 | \hat{C}_n (\hat{H} - E_0 + \omega_n) | \Psi_I^0 \rangle$ in the first term on the RHS of Eq. 207 can be expressed according to

$$\langle\overline{\Psi}_0|\hat{C}_n(\hat{H}-E_0+\omega_n)\hat{C}_I|\Psi_0^{cc}\rangle = -\langle\overline{\Psi}_0|[[\hat{H},\hat{C}_I],\hat{C}_n]|\Psi_0^{cc}\rangle - x_n\omega_n Y_{I0}^* \quad (208)$$

in terms of the double commutator $[[\hat{H},\hat{C}_I],\hat{C}_n]$. Here, we have used the eigenvalue equation for the nth excited state in the form

$$(\hat{H}-E_0)\hat{C}_n|\Psi_0^{cc}\rangle = \omega_n\left(\hat{C}_n|\Psi_0^{cc}\rangle + x_n|\Psi_0^{cc}\rangle\right) \quad (209)$$

Moreover, recall that $\langle\overline{\Psi}_0|\hat{C}_I|\Psi_0^{cc}\rangle = Y_{I0}^*$ and the operators $\hat{C}_n$ and $\hat{C}_I$ commute. Inserting Eq. 208 on the RHS of Eq. 207 constitutes the final step in the reformulation of $\langle\overline{\Psi}_0|\hat{C}_n\hat{D}|\Psi_0^{cc}\rangle$. Using this result in Eqs. 207 and 203, respectively, validates the second term in the CCLR expression (201), but also introduces a third x_n-term,

$$-x_n\omega_n\sum_{I,J}Y_{I0}^*(\boldsymbol{M}+\omega_n)_{IJ}^{-1}\langle\overline{\Phi}_J|\hat{D}|\Psi_0^{cc}\rangle \quad (210)$$

due to the second term on the RHS of Eq. 208. It remains to show that the three x_n terms cancel each other, that is,

$$\langle\overline{\Psi}_0|\hat{D}|\Psi_0^{cc}\rangle - \langle\Phi_0|\hat{D}|\Psi_0^{cc}\rangle - \sum_J\omega_n w_{nJ}\langle\overline{\Phi}_J|\hat{D}|\Psi_0^{cc}\rangle - \omega_n\sum_{I,J}Y_{I0}^*(\boldsymbol{M}+\omega_n)_{IJ}^{-1}\langle\overline{\Phi}_J|\hat{D}|\Psi_0^{cc}\rangle = 0 \quad (211)$$

where the contributions 1, 2 + 3 and 4 on the LHS arise from Eqs. 203, 207 and 210, respectively. The contributions 3 and 4 can be combined and further evaluated in a compact matrix notation as follows:

$$\omega_n(\underline{w}^t+\underline{Y}_0^\dagger)(\boldsymbol{M}+\omega_n)^{-1} = \omega_n(-\omega_n^{-1}\underline{v}^t(\boldsymbol{M}+\omega_n)^{-1} - \underline{v}^t\boldsymbol{M}^{-1}(\boldsymbol{M}+\omega_n)^{-1}) \quad (212)$$

$$= -\omega_n\underline{v}^t(\omega_n^{-1}+\boldsymbol{M}^{-1})(\boldsymbol{M}+\omega_n)^{-1} \quad (213)$$

$$= -\omega_n\underline{v}^t\omega_n^{-1}\boldsymbol{M}^{-1}(\boldsymbol{M}+\omega_n)(\boldsymbol{M}+\omega_n)^{-1} \quad (214)$$

$$= -\underline{v}^t\boldsymbol{M}^{-1} = \underline{Y}_0^\dagger \quad (215)$$

As a result, the sum of the three x_n terms becomes

$$x_n\{\langle\overline{\Psi}_0|\hat{D}|\Psi_0^{cc}\rangle - \langle\Phi_0|\hat{D}|\Psi_0^{cc}\rangle - \sum Y_{J0}^*\langle\overline{\Phi}_J|\hat{D}|\Psi_0^{cc}\rangle\} = 0 \quad (216)$$

where the cancellation now is obvious, as $\langle\overline{\Psi}_0| = \langle\Phi_0| + \sum Y_{J0}^*\langle\overline{\Phi}_J|$.

Excited-state transition moments

In a similar way, one may show the equivalence of the ordinary bCC and the CCLR expressions for excited-state transition moments and properties, the latter reading (Eq. 121)

$$T_{nm} = \langle\overline{\Psi}_n^{(l)}|[\hat{D},\hat{C}_m]|\Psi_0^{cc}\rangle - \sum_{I,J}\langle\overline{\Psi}_n^{(l)}|[[\hat{H},\hat{C}_I],\hat{C}_m]|\Psi_0^{cc}\rangle \times(\boldsymbol{M}+\omega_{mn})_{IJ}^{-1}\langle\overline{\Phi}_J|\hat{D}|\Psi_0^{cc}\rangle + \delta_{nm}\langle\overline{\Psi}_0|\hat{D}|\Psi_0^{cc}\rangle \quad (217)$$

where $\omega_{mn} = \omega_m - \omega_n$. As above, we start from the ordinary bCC expression (100)

$$T_{nm} = \langle\overline{\Psi}_n^{(l)}|\hat{D}\hat{C}_m|\Psi_0^{cc}\rangle + x_m\langle\overline{\Psi}_n^{(l)}|\hat{D}|\Psi_0^{cc}\rangle \quad (218)$$

and use the commutator relation $\hat{D}\hat{C}_m = [\hat{D},\hat{C}_m] + \hat{C}_m\hat{D}$ yielding

$$T_{nm} = \langle\overline{\Psi}_n^{(l)}|[\hat{D},\hat{C}_m]|\Psi_0^{cc}\rangle + \langle\overline{\Psi}_n^{(l)}|\hat{C}_m\hat{D}|\Psi_0^{cc}\rangle + x_m\langle\overline{\Psi}_n^{(l)}|\hat{D}|\Psi_0^{cc}\rangle \quad (219)$$

Analogously to Eq. 204, we consider the identity

$$\langle\overline{\Psi}_n^{(l)}|\hat{C}_m\hat{D}|\Psi_0^{cc}\rangle = \langle\overline{\Psi}_n^{(l)}|\hat{C}_m(\hat{H}-E_0+\omega_{mn})(\hat{H}-E_0+\omega_{mn})^{-1}\hat{D}|\Psi_0^{cc}\rangle \quad (220)$$

and use the the bCC representation of $(\hat{H}-E_0+\omega_{mn})^{-1}$ to further evaluate the RHS. Note that the only difference to Eqs. 205 and 206 is the replacement of ω_n by ω_{mn}. This leads to

$$\langle\overline{\Psi}_n^{(l)}|\hat{C}_m\hat{D}|\Psi_0^{cc}\rangle = \sum_{I,J}\langle\overline{\Psi}_n^{(l)}|\hat{C}_m(\hat{H}-E_0+\omega_{mn})|\Psi_I^0\rangle(\boldsymbol{M}+\omega_{mn})_{IJ}^{-1}\langle\overline{\Phi}_J|\hat{D}|\Psi_0^{cc}\rangle + \delta_{mn}(\langle\Phi_0|\hat{D}|\Psi_0^{cc}\rangle - \sum_{I,J}v_I(\boldsymbol{M}+\omega_{mn})_{IJ}^{-1}\langle\overline{\Phi}_J|\hat{D}|\Psi_0^{cc}\rangle) \quad (221)$$

using here $\langle\overline{\Psi}_n^{(l)}|\hat{C}_m|\Psi_0^{cc}\rangle = \delta_{mn}$. Let us consider the second term on the RHS, which is non-vanishing only for $n = m$ due to the Kronecker symbol. Since $\omega_{mn} = 0$ for $m = n$, and

$$\underline{v}^t\boldsymbol{M}^{-1} = -\underline{Y}_0^\dagger \quad (222)$$

the latter term becomes $\delta_{mn}\langle\overline{\Psi}_0|\hat{D}|\Psi_0^{cc}\rangle$, thus reproducing the third term in the CCLR expression (217). As in Eq. 208, we now may introduce a double commutator according to

$$\langle\overline{\Psi}_n^{(l)}|\hat{C}_m(\hat{H}-E_0+\omega_{mn})\hat{C}_I|\Psi_0^{cc}\rangle = -\langle\overline{\Psi}_n^{(l)}|[[\hat{H},\hat{C}_I],\hat{C}_m]|\Psi_0^{cc}\rangle - x_m\omega_m Y_{In}^* \quad (223)$$

Here, we have used the eigenvector equation for the mth excited state in the form

$$(\hat{H}-E_0)\hat{C}_m|\Psi_0^{cc}\rangle = \omega_m(\hat{C}_m|\Psi_0^{cc}\rangle + x_m|\Psi_0^{cc}\rangle) \quad (224)$$

and the relations $\langle\overline{\Psi}_n^{(l)}|\hat{C}_I|\Psi_0^{cc}\rangle = Y_{In}^*$ for the left eigenvector components. Using this result in Eq. 221 gives

$$\begin{aligned}\langle\overline{\Psi}_n^{(l)}|\hat{C}_m\hat{D}|\Psi_0^{\rm cc}\rangle &= -\sum_{I,J}\langle\overline{\Psi}_n^{(l)}|[[\hat{H},\hat{C}_I],\hat{C}_m]|\Psi_0^{\rm cc}\rangle(\boldsymbol{M}+\omega_{mn})^{-1}_{IJ}\langle\overline{\Phi}_J|\hat{D}|\Psi_0^{\rm cc}\rangle \\ &\quad - x_m\omega_m\sum_{I,J}Y^*_{In}(\boldsymbol{M}+\omega_{mn})^{-1}_{IJ}\langle\overline{\Phi}_J|\hat{D}|\Psi_0^{\rm cc}\rangle\end{aligned} \tag{225}$$

The first term on the RHS is seen to reproduce, via Eq. 219, the second term of the CCLR expression (217). It remains to inspect the second term on the RHS, containing the factor x_m. Since $\underline{Y}_n$ is a left eigenvector of $\boldsymbol{M}$, it follows that

$$\underline{Y}_n^\dagger(\boldsymbol{M}+\omega_{mn})^{-1} = (\omega_n+\omega_{mn})^{-1}\underline{Y}_n^\dagger = \omega_m^{-1}\underline{Y}_n^\dagger \tag{226}$$

Thus,

$$\begin{aligned}&-x_m\omega_m\sum_{I,J}Y^*_{In}(\boldsymbol{M}+\omega_{mn})^{-1}_{IJ}\langle\overline{\Phi}_J|\hat{D}|\Psi_0^{\rm cc}\rangle \\ &\quad = -x_m\langle\overline{\Psi}_n^{(l)}|\hat{D}|\Psi_0^{\rm cc}\rangle\end{aligned} \tag{227}$$

which cancels the original x_m term on the RHS of Eq. 219. This concludes our proof.

References

1. Coester F (1958) Nucl Phys 7:421
2. Cízek J (1966) J Phys Chem 45:4256
3. Cízek J (1969) Adv Chem Phys 14:35
4. Monkhorst HJ (1977) Int J Quantum Chem Symp 11:421
5. Dalgaard E, Monkhorst HJ (1983) Phys Rev A 28:1217
6. Takahashi M, Paldus J (1986) J Chem Phys 85:1486
7. Koch H, Jørgensen P (1990) J Chem Phys 93:3333
8. Koch H, Jensen HJA, Jørgensen P, Helgaker T (1990) J Chem Phys 93:3345
9. Paldus J, Cízek J, Saute M, Laforgue A (1978) Phys Rev A 17:805
10. Mukherjee D, Mukherjee PK (1979) Chem Phys 39:325
11. Ghosh S, Mukherjee D, Bhattacheryya D (1982) Chem Phys 72:161
12. Sekino H, Bartlett RJ (1984) Int J Quantum Chem Symp 18:255
13. Geertsen J, Rittby M, Bartlett RJ (1989) Chem Phys Lett 164:57
14. Stanton JF, Bartlett RJ (1993) J Chem Phys 98:7029
15. Nakatsuji H, Hirao K (1977) Chem Phys Lett 47:569
16. Nakatsuji H (1979) Chem Phys Lett 67:329
17. Nakatsuji H (1979) Chem Phys Lett 67:334
18. Mertins F, Schirmer J (1996) Phys Rev A 53:2140
19. Koch H, Kobayashi R, de Merás AS, Jørgensen P (1994) J Chem Phys 100:4393
20. Christiansen O, Koch H, Jørgensen P (1996) J Chem Phys 105:1451
21. Hald K, Jørgensen P, Olsen J, Jaszuński M (2001) J Chem Phys 115:671
22. Mukhopadhyay D, Mukhopadhyay S, Chauduri R, Mukherjee D (1991) Theor Chim Acta 80:441
23. Stanton JF (1994) J Chem Phys 101:8928
24. Trofimov AB, Stelter G, Schirmer J (1999) J Chem Phys 111:9982
25. Schirmer J (1982) Phys Rev A 26:2395
26. Trofimov AB, Schirmer J (1995) J Phys B 28:2299
27. Meunier A, Levy B (1979) Int J Quantum Chem 16:955
28. Helgaker T, Jørgensen P, Olsen J (2000) Molecular electronic structure theory. Wiley, New York
29. Kutzelnigg W (1991) Theor Chim Acta 80:349
30. Szalay PG, Nooijen M, Bartlett RJ (1995) J Chem Phys 103:281
31. Christiansen O, Koch H, Jørgensen P (1995) J Chem Phys 103:7429
32. Schirmer J, Trofimov AB (2004) J Chem Phys 120:11449
33. Fetter AL, Walecka JD (1971) Quantum theory of many-particle systems. Mc Graw-Hill, New York
34. Schirmer J, Mertins F (1996) Int J Quantum Chem 58:329
35. Hättig C (2005) Adv Quantum Chem 50:37
36. Köhn A, Tajti A (2007) J Chem Phys 127:044105
37. Ghosh S, Mukherjee D, Bhattacheryya D (1981) Mol Phys 43:173
38. Stanton JF, Gauss J (1994) J Chem Phys 101:8938
39. Nooijen M, Bartlett RJ (1995) J Chem Phys 102:3629
40. Hirata S, Nooijen M, Bartlett RJ (2000) Chem Phys Lett 328:459
41. Bartlett RJ, Musial M (2007) Rev Mod Phys 79:291
42. Lindgren I (1979) Int J Quantum Chem Symp 12:3827
43. Hose G, Kaldor U (1979) J Phys B 12:3827
44. Jeziorski B, Monkhorst HJ (1981) Phys Rev A 24:1668
45. Haque M, Mukherjee D (1984) J Chem Phys 80:5058
46. Lindgren I, Mukherjee D (1987) Phys Rep 151:93
47. Pal S, Rittby M, Bartlett RJ, Sinha D, Mukherjee D (1988) J Chem Phys 88:4357
48. Mukherjee D, Pal S (1989) Adv Quantum Chem 20:561
49. Hubbard J (1957) Proc R Soc A 240:539